geosciences

MDPI

Article

Features That Favor the Prediction of the Emplacement Location of Maar Volcanoes: A Case Study in the Central Andes, Northern Chile

Gabriel Ureta [1,2,3], Károly Németh [4,*], Felipe Aguilera [1,3,5] and Rodrigo González [1,5]

1 Núcleo de Investigación en Riesgo Volcánico Ckelar Volcanes, Universidad Católica del Norte, Av. Angamos 0610, Antofagasta 1270709, Chile; gabriel.ureta@ucn.cl (G.U.); feaguilera@ucn.cl (F.A.); r_gonzalez@ucn.cl (R.G.)
2 Programa de Doctorado en Ciencias Mención Geología, Universidad Católica del Norte, Av. Angamos 0610, Antofagasta 1270709, Chile
3 Centro Nacional de Investigación para la Gestión Integrada del Riesgo de Desastres (CIGIDEN), Av. Vicuña Mackenna 4860, Santiago 7820436, Chile
4 Volcanic Risk Solutions, School of Agriculture and Environment, Massey University, Palmerston North 4442, New Zealand
5 Departamento de Ciencias Geológicas, Universidad Católica del Norte, Av. Angamos 0610, Antofagasta 1270709, Chile
* Correspondence: k.nemeth@massey.ac.nz; Tel.: +64-27-479-1484

Received: 13 October 2020; Accepted: 18 December 2020; Published: 21 December 2020

Abstract: Maar volcanoes are monogenetic landforms whose craters cut below the pre-eruptive surface and are surrounded by a tephra ring. Both the maar crater and the surrounding tephra rim deposits are typically formed due to magma–water explosive interactions. Northern Chile is located in the Central Volcanic Zone of the Andes where, in literature, 14 maars have been recognized as parasite (6) and individual (8) volcanoes. Amongst these individual maars, 3 of them, namely the Tilocálar Sur, Cerro Tujle, and Cerro Overo volcanoes, are not related to calderas and were emplaced <1 Ma ago by magmatic explosive-effusive and phreatomagmatic eruptions. Based on the evolution and control of the volcanic eruptive styles of these three maars, which have been determined in previous research through fieldwork, stratigraphic, morphometric, textural (density and vesicularity), petrographic, and geochemical analyses, a set of key features that favor a prediction of the emplacement location of maar volcanoes in Central Andes, northern Chile are proposed. The set of features that permit and favor the growth mechanisms for maar formations corresponds to (i) a compressive tectonic setting (e.g., ridge structures), (ii) groundwater recharge (e.g., snowmelt and seasonal rainfall), (iii) the lithological setting (e.g., layers of low permeability), (iv) the presence of aquifer and/or endorheic basins (e.g., lakes or salars), and (v) a period of stress relaxation that permits magma ascent to the surface in volcanically active areas. Considering these characteristics, it is possible to identify places where phreatomagmatic eruption can occur. If the magma ascent flux is lower than the groundwater flux, this can lead to a phreatomagmatic eruption because of groundwater coming into contact with the magma. These eruptive features evidence internal—and external—factors that play an essential role in the transition from explosive-effusive magmatic to phreatomagmatic volcanic eruption styles during the same eruptive period that is one of the biggest challenges in volcanic hazard evaluations. Although, in this contribution, a set of features that permit and favor the growth mechanisms for a prediction of the emplacement location of maars in northern Chile is proposed, these considerations could also be applied to identify potential locations in other parts of the world where magma–water interaction eruption could occur. Therefore, this approach could be useful in the prediction of hydromagmatic volcanic eruptions and, thus, in mitigating the impact of volcanic hazard for the inhabitants of the surrounding areas.

Keywords: Altiplano-Puna; monogenetic volcanoes; phreatomagmatism; Tilocálar Sur maar; Cerro Tujle maar; Cerro Overo maar

1. Introduction

Maar volcanoes are the second most abundant type of volcanoes on continents and islands after scoria cones [1,2]. They can occur in any tectonic setting and are found isolated in monogenetic volcanic fields or associated with polygenetic volcanoes [3]. They are small-volume volcanic edifices, characterized by a hole-in-the-ground morphology where its floor is below the pre-eruptive surface surround by a tephra ring deposit [4]. Maar volcanoes are characterized by small-volume, short eruptive duration, typically associated with a simple magmatic plumbing system, ranging from simple to complex eruptive morphology (number of explosions) and from basaltic to rhyolitic composition [4–18]. They are typically the result of externally-driven fragmentation when the melt interacts directly with external water (e.g., seawater, water-saturated sediments, lakes, groundwater table, littoral cone, or rootless cone). This direct interaction between magma and water is known as phreatomagmatic or Taalian eruption which forms one of the most common subaerial volcanic crater types of explosive volcanism such as maar-diatremes [1,11,15,18]. In addition, maar volcanoes can display a complex architecture of the volcanic edifice that is determined by the number of eruptions and type of eruption styles [11,19]. In this context, they typically transition from phreatomagmatic to magmatic eruptions, evidenced by the final volcanic landforms as maar-diatremes associated with a lava dome (e.g., [20]), lava flows (e.g., [21]), or scoria cones (e.g., [21]). There are few cases where monogenetic volcanoes were formed by a magmatic eruption and then destroyed by a phreatomagmatic eruption at a later stage, and evidence of an actual transition from magmatic to hydromagmatic eruptions is found in cases such as Crater Elegante, Mexico [22,23], Halema'uma'u 1924, Hawaii [24–26], Al Haruj al Abyad, Libya [27], Alumbrera scoria cone, Argentina [28], or Dotsero volcano, Colorado, USA [29]. Confirmation of the presence or absence of phreatomagmatism and the role of the water in the formation of maars has been proven in many studies e.g., [15,30,31]. The diagnostic criteria are the typical features described for ultrabasic and basic maars studied worldwide and for the current models on the phreatomagmatic emplacement of maar-diatreme volcanoes in subaerial continental environments [6,8,9,32]. Nevertheless, for intermediate maars, the criteria to distinguish magmatic versus phreatomagmatic tend to be ambiguous or have exceptions, concerning the typical features of emplacement models of ultrabasic and basic maars.

In the Central Volcanic Zone of the Andes, a total of 14 volcanoes have been defined as maars in northern Chile [33] as parasite (volcanic features forming vents, craters, cones, domes, and mounds of varying diameter and height situated either beside the main cones or at the flanks and bases of volcanoes; [34]) and individual centers (Figure 1). Parasite maar volcanoes correspond to Alitar [35], Puntas Negras [36], El Laco Sur [37], Juan de la Vega [38], Baker [35], and La Espinilla [39]. Individual maar volcanoes are Michacollo [40], Lliza [40], Churullo [41], Cerro Jarellón or Pampa Redonda [42–44], Corral de Coquena [42–46], Cerro Overo [35,47–49], Cerro Tujle [47,48,50], and Tilocálar Sur [47,48,51]. Nevertheless, most of these centers have been defined as maar in the pure morphological sense (e.g., a broad flat-floored crater that cuts into the syn-eruptive surface) regardless of whether these were formed by a direct magma–water interaction (maar volcano; [4]), or by an indirect magma water interaction vaporized by heat without direct contact with fresh magma (explosion crater or hydrothermal explosion pit; [52]).

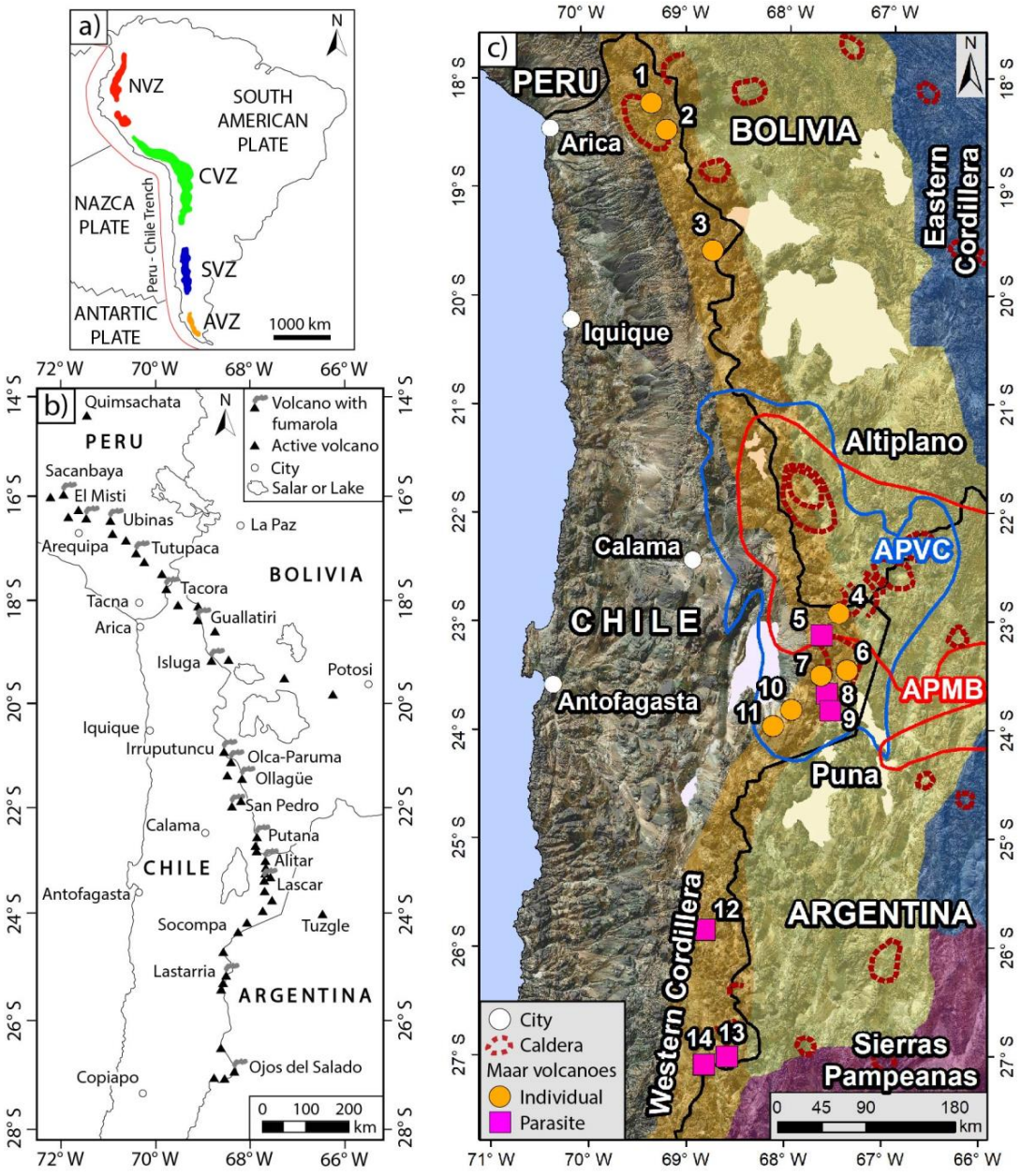

Figure 1. Location maps. (**a**) Map showing the location of the Northern, Southern, Central, and Austral Volcanic Zones (NVZ, CVZ, SVZ, and AVZ, respectively) of the Andes defined by Thorpe and Francis [55] (Modified from [36]). (**b**) Location map of the CVZ (Modified from [36]) showing the main active polygenetic volcanoes [56]. (**c**) Map of northern Chile showing the location of the maar volcanoes in northern Chile and major morpho-volcano-tectonic units of the Central Andes (Modified from [57–59]). (APVC) Altiplano-Puna Volcanic Complex; (APMB) Altiplano-Puna Magma Body; (1) Michacollo; (2) Lliza; (3) Churullo; (4) Jorullo or Pampa Redonda; (5) Alitar; (6) Corral de Coquena; (7) Cerro Overo; (8) Puntas Negras; (9) El Laco Sur; (10) Cerro Tujle; (11) Tilocálar Sur; (12) Juan de la Vega; (13) Baker; (14) La Espinilla.

The main objective of this study is to describe the potential features that favor the prediction of the emplacement location of maar volcanoes in Central Andes, northern Chile, in order to determine an emplacement model for intermediate maar volcanoes by magma–water interaction (phreatomagmatism). Based on detailed field observations of the maar deposits such as lithologies and features of erupted material, Ureta, et al. [50], Ureta, et al. [53], and Ureta, et al. [54] described the eruptive evolution of the Cerro Tujle maar, Tilocálar Sur maar, and the Cerro Overo maar, respectively. They highlighted the stratigraphy, morphometry, petrography, and geochemistry in order to reconstruct

the evolution of these maar-craters within the context of their eruptive events. However, many aspects of the sequential organization of the eruptive products and their causal relationship with the eruptive mechanism remain obscure especially from a regional perspective. Such information would be necessary, as this would limit probable settings that favor the occurrence of phreatomagmatic eruptions, providing insight into the eruptive conditions that trigger magma–water interaction during magma ascent to the surface. In this context, this contribution is a standalone critical statement based on the descriptive works developed by Ureta, et al. [50] in Cerro Tujle maar, Ureta, et al. [53] in Tilocálar Sur maar, and Ureta, et al. [54] in Cerro Overo maar. This contribution presents a set of key features that allow and favor the recognition of the location of growth and fragmentation of the phreatomagmatic eruptions that form the maar volcanoes in northern Chile. These conditions that favor phreatomagmatism are based on a link between the transition from magmatic explosive-effusive to hydromagmatic eruption-driven styles at maars which could be applied in other settings around the world such as the Altiplano-Puna region. An additional goal of this study is to contribute to volcanic hazard assessment associated with hydrovolcanic eruptions.

2. Geological and Volcanological Setting

The Andean Cordillera presents more than 200 Pleistocene and Holocene volcanoes forming a >7500 km long morphologically continuous mountain chain along the westerns margin of South America which is divided into four segments i.e., the Northern, Central, Southern, and Austral volcanic zones [36,60,61]. Northern Chile is located in the Central Volcanic Zone (CVZ), extending from latitude 14° S to 28° S [36,55,62]. The origin of this volcanism in the CVZ is a consequence of the changes in the subduction angle of the Nazca Plate (25–30°) below the South American Plate at depths > 400 km at a rate of 68–80 mm/yr [60,63,64]. In this sense, Andean magmatism is driven by the dehydration of the subducted oceanic lithosphere, resulting in melting of the overlying mantle wedge [61,65]. Magmas generated at CVZ that derive from such mantle will be underplated at the crust base and thus able to experience assimilation, fractional crystallization, mixing/mingling during subsequent rise through the crust [55,65–67]. An exceptionally thick continental crust characterizes this volcanic zone from >70 km (below western Cordillera) to ~55 km (south of Puna plateau) and resulted from tectonic shorting [68–70] during the last 10 Ma. Most of the Pleistocene and Holocene volcanism in the CVZ of northern Chile occurs on a high central plateau at an elevation of 3700 to 4500 m a.s.l. with numerous stratovolcanoes of peaks reaching >6000 m elevation [68–70]. This segment is the most apparent expression along the western boundary of two morphotectonic regions, Altiplano (15–23° S) and Puna (23–28° S) [36]. Volcanism in the CVZ during crustal thickening represents one of the largest ignimbrite provinces on the Earth [71], producing numerous polygenetic or stratovolcanoes, and more rarely, isolated monogenetic centers [35,36].

3. Case Studies

Among the 14 maar volcanoes identified in northern Chile (3 Miocene; 4 Pliocene; 5 Pleistocene; 2 Holocene; [33]), 7 of them correspond to individual centers of which 3 of them are from Pleistocene, not associated with caldera systems, and display similar magma composition of the Altiplano-Puna Volcanic Complex [59]. These are the maars known as Tilocálar Sur, Cerro Tujle, and Cerro Overo (Figure 2). The main field observation, stratigraphic, morphological, petrographic, and geochemical features of these three maar volcanoes were taken from previous works such as Ureta, et al. [53] for Tilocálar Sur maar, Ureta, et al. [50] for Cerro Tujle maar, and Ureta, et al. [54] for Cerro Overo maar and are summarized in Tables 1–3.

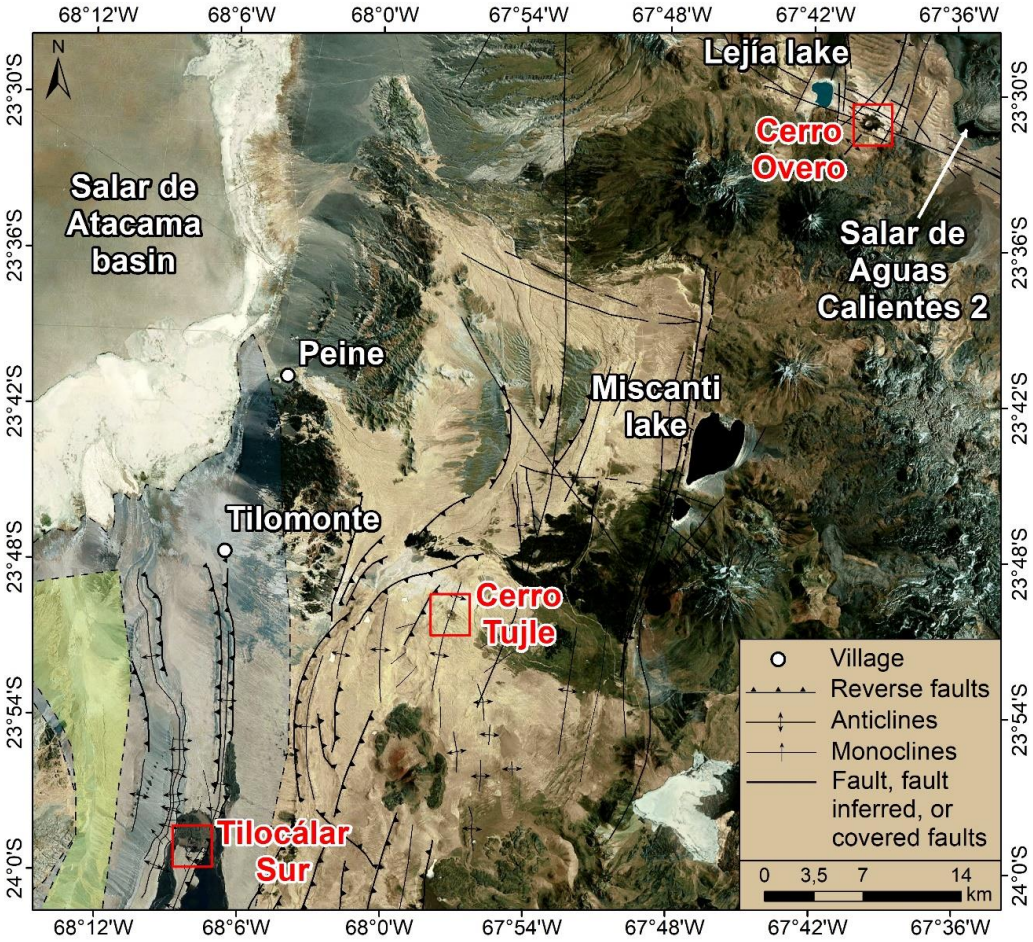

Figure 2. The location map of the Tilocálar Sur, Cerro Tujle, and Cerro Overo maars (red squares) is based on a satellite image acquired from Google Earth™. The light blue area corresponds to the Monturaqui–Negrillar–Tilopozo (MNT) aquifer boundary, whereas the light green area indicates the Tilopozo wetland, which is considered as the discharge point for the groundwater coming from the MNT aquifer into the Salar de Atacama (modified from [72]). The structural features were taken from Ramírez and Gardeweg [48], Kuhn [73], Aron [74], and González, et al. [75].

Table 1. General features of Tilocálar Sur, Cerro Tujle, and Cerro Overo maars.

Maar-Ejecta Ring	Tilocálar Sur [1]	Cerro Tujle [2]	Cerro Overo [3]
Whole-rock composition	Andesite	Andesite	Basaltic andesite
Average envelope density	1.17 (gr/cm^3)	2.45 (gr/cm^3)	2.84 (gr/cm^3)
Mineral assemblage	Ol, Pl, Opx, Cpx, Sd, Qz	Ol, Pl, Opx, Cpx	Ol, Pl, Sp, Cpx, Qz
Water Source	Groundwater (Monturaqui-Negrillar-Tilopozo aquifer)	Groundwater (Related to Salar de Atacama)	Groundwater (Related to Laguna Lejía)
Substrate type	Low permeability ignimbrite layers filled with recent permeable volcanic and sedimentary units	Low permeability ignimbrite layers filled with recent permeable volcanic and sedimentary units	Low permeability ignimbrite layers filled with recent permeable volcanic-derived sediments
Number of eruptive phases	(1) phreato-Strombolian	(1) magmatic effusive, (1) phreatomagmatic	(1) magmatic explosive, (1) magmatic effusive, (1) phreatomagmatic
Type of eruptive styles	phreato-Strombolian	Strombolian and phreatomagmatic	Strombolian and phreatomagmatic

[1] Ureta, et al. [53]; [2] Ureta, et al. [50]; [3] Ureta, et al. [54]. Olivine (Ol), Plagioclase (Pl), Orthopyroxene (Opx), Clinopyroxene (Cpx), Sideromelane (Sd), Qz (Quartz), Spinel (Sp).

Table 2. Morphometric characteristics of Tilocálar Sur, Cerro Tujle, and Cerro Overo maars.

Maar-Ejecta Ring	Tilocálar Sur [1]	Cerro Tujle [2]	Cerro Overo [3]
Bulk volume current crater cavity (m^3)	1.32×10^6	1.46×10^6	6.52×10^6
Bulk volume of tephra deposit (m^3)	not calculated	3.91×10^5	21.20×10^5
DRE volume of tephra deposit (m^3)	not calculated	1.53×10^5	5.19×10^5
Area of tephra deposit (m^2)	not calculated	4.30×10^5	20.20×10^5
Maximum crater diameter (m)	380	333	580
Minimum crater diameter (m)	294	279	480
Current crater depth (m)	34	73	72
Maximum theoretical crater depth (m) [a]	299	141	89
The dip of the outer ring (°)	−5	6	18
The dip of the inner ring (°)	59	70	60
The theoretical aperture of the cone [b]	62	40	60

[1] Ureta, et al. [53]; [2] Ureta, et al. [50]; [3] Ureta, et al. [54]. [a] Maximum theoretical crater depth = Maximum ratio × SENO (Dip inner ring)/SENO (Theoretical aperture of the cone/2). [b] Theoretical aperture of the cone = 2 × (90 − Dip inner ring).

Table 3. Deposit features of Tilocálar Sur, Cerro Tujle, and Cerro Overo maars.

Maar-Ejecta Ring	Tilocálar Sur [1]	Cerro Tujle [2]	Cerro Overo [3]
Color of deposit	Brown reddish	Brown reddish	Black
Dominant stratification	Plane parallel bedded	Plane parallel bedded	Plane parallel bedded, cross-lamination
Dominant grain size	Lapilli	Lapilli	Lapilli
The average thickness of deposit (m)	not calculated	0.6	0.7
Mode of emplacement	Fall out	Surge and fall out	Surge and fall out
Degree of sorting	Poor	Variable	Moderate
Agglutination/welding	No	No	No
Dominant lithic grain size	Coarse lapilli to bomb/block	Coarse lapilli to bomb/block	Fine lapilli to bomb/block
Accretionary lapilli	No	No	No
Ballistic impact	No	No	Yes (ignimbrite and black lava)
Ballistic fragments	Yes (ignimbrite, conglomerate, volcanic rock, intrusive rocks)	Yes (ignimbrite, lava)	Yes (ignimbrite, intrusive rocks, black lava)
Type of recycled juvenile	Yes (scoria and agglutinated material)	Yes (grey lava)	Yes (black lava)
Breccia with juvenile	Yes (limited)	Yes (limited)	Yes (moderate)
Lithic content (vol.%)	10	38	71
Type of juvenile pyroclast fragment	Scoria	Scoria	Scoria
Dominant juvenile pyroclast grain size	Coarse lapilli	Fine lapilli	Ash to Coarse lapilli
Juvenile pyroclast content (vol.%)	77	44	14
Juvenile pyroclast vesicularity (%)	59	11	38
Size of vesicle	Medium to small	Small	Small
Juvenile pyroclast morphology	Cauliflower, chilling border	Cauliflower, chilling border	Cauliflower, chilling border, bread-crust
Juvenile pyroclast shape	Mainly scoria, the shape is controlled by vesicles	Angular/blocky to irregular	Angular/blocky to irregular/amoeboid

[1] Ureta, et al. [53]; [2] Ureta, et al. [50]; [3] Ureta, et al. [54].

3.1. Tilocálar Sur Maar

According to Ureta, et al. [53], this maar displays a crater (Figure 3) of 380 × 294 m; the depth reaches 34 m, and an erupted bulk volume of 0.0025 km^3. The syn-eruptive landscape level of this crater corresponds to the Tucúcaro Ignimbrite which is covered by a pyroclastic fall deposit of basaltic andesite to andesite composition (55–62 SiO_2 wt.%) from the Tilocálar Sur volcano. Individual rock fragments are present around the crater rim corresponding to scoriaceous material (ash and lapilli) with cauliflower texture, cooling cracks, chilled margins, and fragments from the Tilocálar Sur pyroclastic fall deposit, Tucúcaro Ignimbrite, volcanic, sedimentary, and granitic rocks (basement).

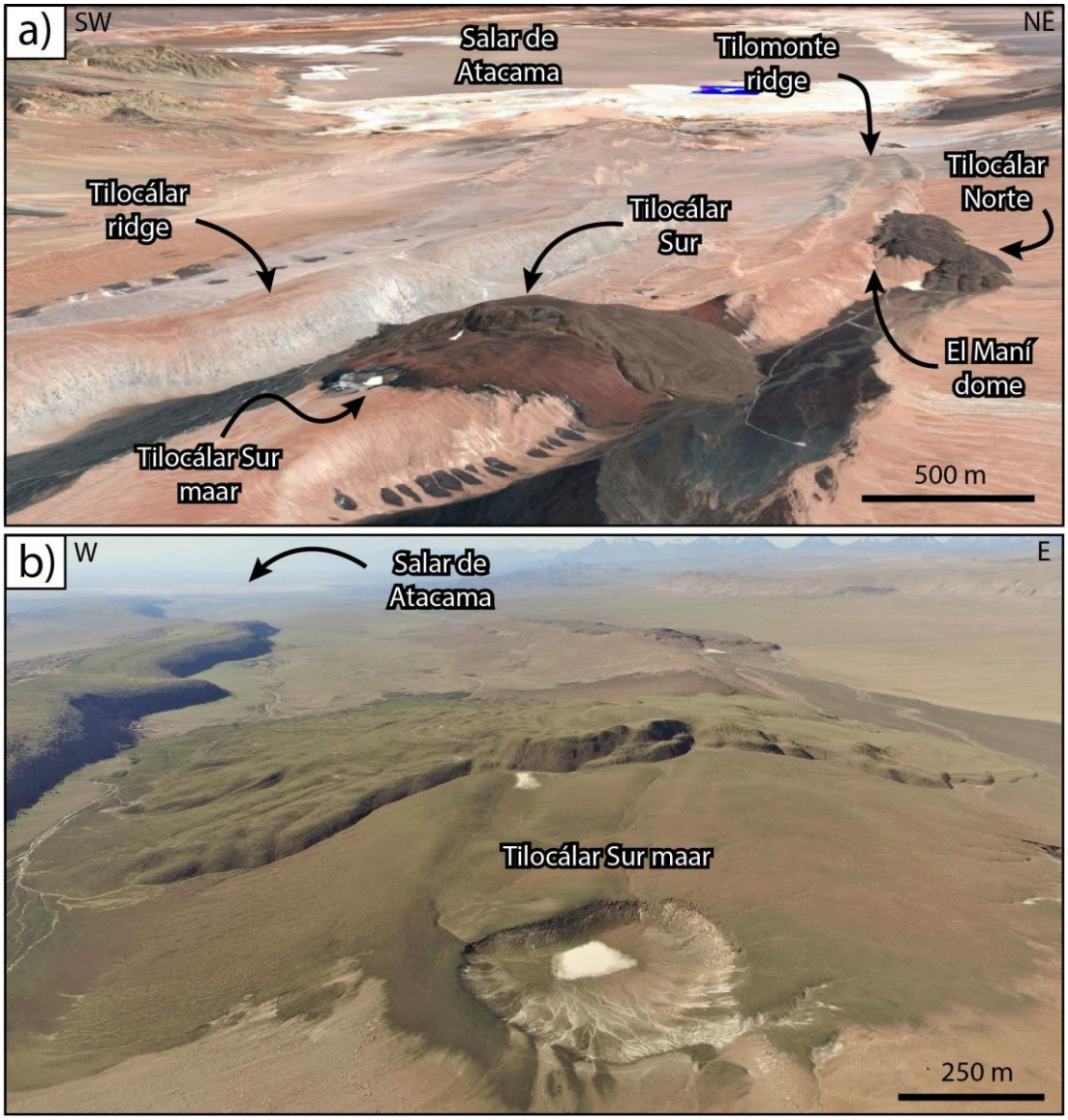

Figure 3. Tilocálar Sur maar. (**a**) Satellite image taken from Google Earth™, showing the location of the Salar de Atacama basin and the morphology of the surface. (**b**) Aerial view of the Tilocálar Sur maar.

3.2. Cerro Tujle Maar

A similar kind of deposit is observed near the rim of Cerro Tujle maar (Figure 4). According to Ureta, et al. [50], the deposit has an andesitic composition (56–58 SiO_2 wt.%) which consists of a lower andesitic lava flow that is emplaced over the Tucúcaro Ignimbrite and an upper pyroclastic deposit characterized mainly by lapilli and block/bomb fragments with dacitic to rhyolitic xenoliths. Breccia

fragments with lithic and juvenile clasts are also to be found. Cerro Tujle has an elliptical crater of 333 × 279 m, with a depth reaching to 73 m. The crater's cavity presents a volume of 0.002 km^3 with an estimated erupted bulk volume of 0.024 km^3.

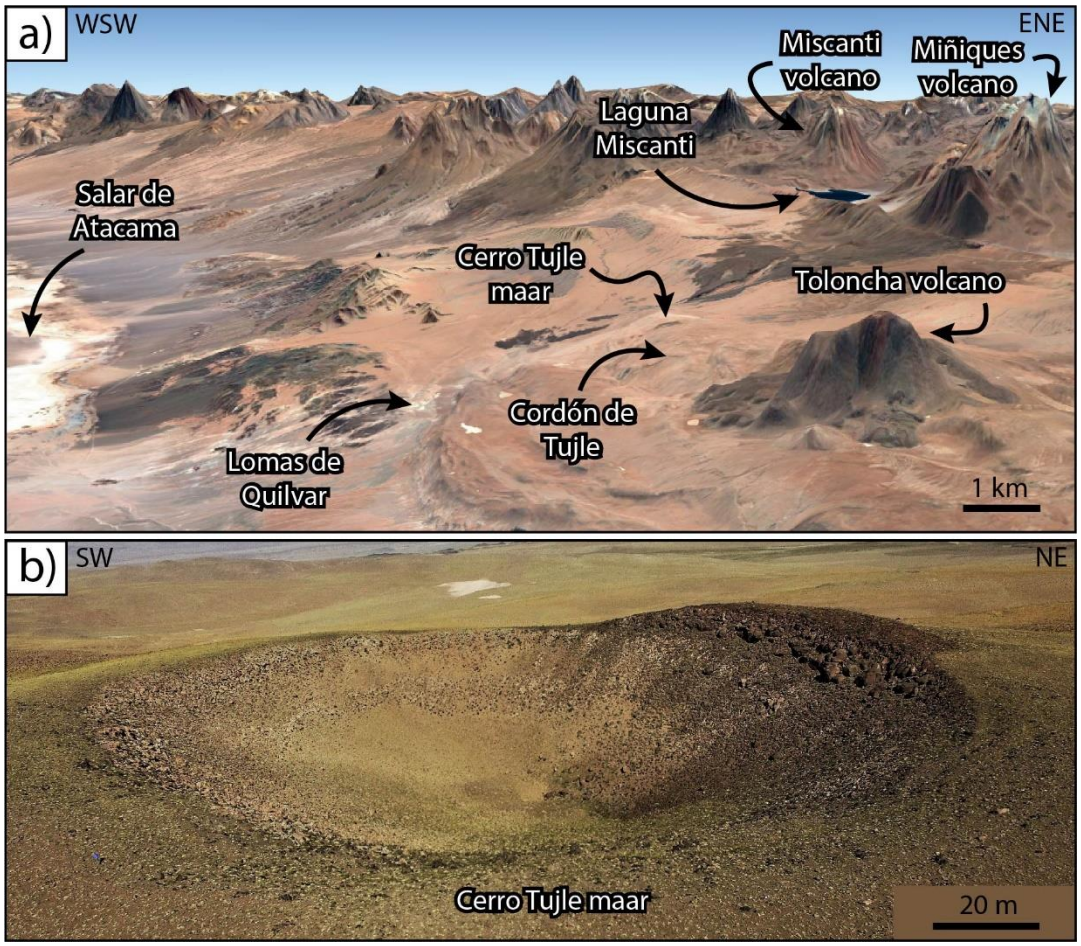

Figure 4. Cerro Tujle maar. (**a**) Satellite image taken from Google Earth™, showing the location of the Salar de Atacama basin, Laguna Miscanti, and the morphology of the surface. (**b**) Aerial view of the Cerro Tujle maar where it is possible to see the andesitic lava unit under the tephra ring.

3.3. Cerro Overo Maar

Cerro Overo (Figure 5) is the least silicic maar yet analyzed from this area [76]. Clasts range in composition from 52 to 56 SiO_2 wt.% [54] where rocks from Cerro Overo are characterized by the presence of olivine and clinopyroxene crystals [47,49,54]. According to Ureta, et al. [54], its crater is 480 × 580 m; its depth reaches 72 m and it has an estimated eruptive volume of 0.0093 km^3, represented by two volcano-stratigraphic units. The first one lies over the Tuyajto and Cajón Ignimbrites and corresponds to pyroclastic and lava deposits with fluid textures and breccia's fragments. In contrast, the second one is a surge deposit that covers the lava unit, characterized by the presence of scoriaceous fragments (ash and lapilli) that present a wide range of vesicularity, cooling cracks, cauliflower textures, chilled margins, and breccia fragments with juvenile material and lithic clasts.

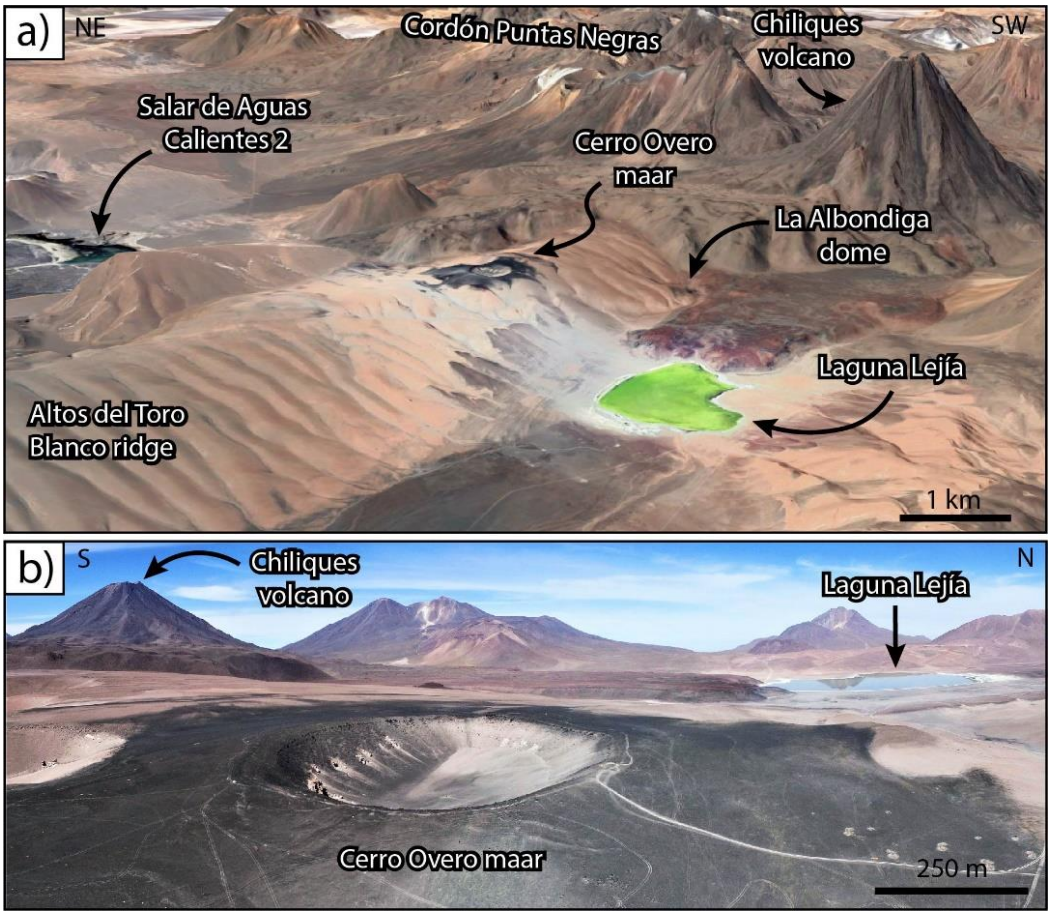

Figure 5. Cerro Overo maar. (**a**) Satellite image taken from Google Earth™, showing the location of the Laguna Lejía, Salar de Aguas Calientes 2, and the morphology of the surface. (**b**) Aerial view of the Cerro Overo maar.

4. Discussion

4.1. Origin of the Phreatomagmatism

Recently, some studies (e.g., [77–79]) argue that maar volcanoes can be produced by the effects of magmatic gases that excavate a vent, followed by continued upward streaming of gas (violent release of CO_2 probably of mantle origin) through vent-filling debris and may not necessarily be a result of magma–water interaction (dry-maar).

The case studies in this work are characterized by their location at a thick crust environment (~70 km; [70]), degree of magma composition that is related to low volatile contents (calc-alkaline basaltic andesite to andesite magma), low number and amount of minerals that can contain water to support crystal growth in a volatile-rich environment (lack of phlogopite and range of Mg#), and low volume of magma batch (<1 km^3).

Although decompression and adiabatic cooling can generate explosive conditions in the initial phase during the eruptive activity of the studied maar volcanoes, the idea of a magma that initially carried large amount of volatiles which were largely released or exsolved during ascent as a result of decompression and adiabatic cooling subsequently generating an explosive condition with sufficient energy to produce a crater at least 500 m in diameter and ~80 m depth is quite unreasonable (e.g., [80,81]).

4.2. The Role of the Eruption Location on Water Availability

Tilocálar Sur, Cerro Tujle, and Cerro Overo maars are located in three different local settings. (i) Tilocálar Sur maar (at 3060 m a.s.l.) is located at a 67 km-thick crust [70], shallow basement corresponds

to volcano-sedimentary units such as the Paciencia and Purilactis Group and Tucúcaro Ignimbrite (moderately welded) where the Monturaqui-Negrillar-Tilopozo aquifer is present (Figures 2 and 3). (ii) Cerro Tujle maar (at 3554 m a.s.l.) lies at a 67 km-thick crust [70], shallow basement corresponds to Tucúcaro and Patao Ignimbrites (moderately welded), this location is on the route of the groundwater levels that feed the Salar de Atacama basin (Figures 2 and 4). (iii) Cerro Overo maar (at 4556 m a.s.l.) is situated at a 59 km-thick crust [70] where the shallow level is dominated by Cajón Ignimbrite (weakly welded) and close to the Laguna Lejía (Figures 2 and 5). Nevertheless, these three maars are positioned at the same location on the same type of tectonic structure, which is the hinge top zone of Tilomonte-, Cerro Tujle- or Toloncha-, and Altos del Toro Blanco- ridges, respectively (Figures 3–5, respectively).

Northern Chile, specifically, the Atacama Desert, is one of the major hyper arid deserts of the world. Despite this, the presence of salt flats or water bodies such as Tilomonte wetland, Salar de Atacama, Laguna Miscanti, Laguna Tuyajto, or Laguna Lejía (Figure 2), among others, is clear and robust evidence of active water feeding recharge and discharge systems controlled by hydrological and hydrogeological aspects in the arid Chilean Altiplano environment (e.g., [82,83]). The sub-surface country-rock has low permeability [48,84–86]. It is defined by the ignimbrite layers consisting of recent permeable pyroclastics where gaps with hydraulic connection are developed [85–88]. This favors different groundwater levels that are mostly shallow (e.g., [89–91]). On the other hand, ridge type structures have been proposed to have resulted from slip along buried faults that have a listric profile, generating flat portions of the faults that may be mechanically controlled by the stratigraphy of the deforming units [74,75]. This suggests that water bodies could be stored at this flat portion of the faults of the Tilomonte-, Cerro Tujle- or Toloncha-, and Altos del Toro Blanco- ridges.

Although the cases studied have not been examined in detail from a hydrological and hydrogeological perspective, the explosion depth range of Tilocálar Sur, Cerro Tujle, and Cerro Overo maars is 33–103 m, 25–35 m, and 41–115 m, respectively [50,53,54] (Figure 6). These ranges are consistent with the thickness and regional extent of the ignimbrite deposits and local tectonic setting, supporting the availability of groundwater levels at these locations. In addition, this spectrum of explosion depths is in the likely range of containment depth for phreatomagmatic explosions, which is in the uppermost ~200 m [92].

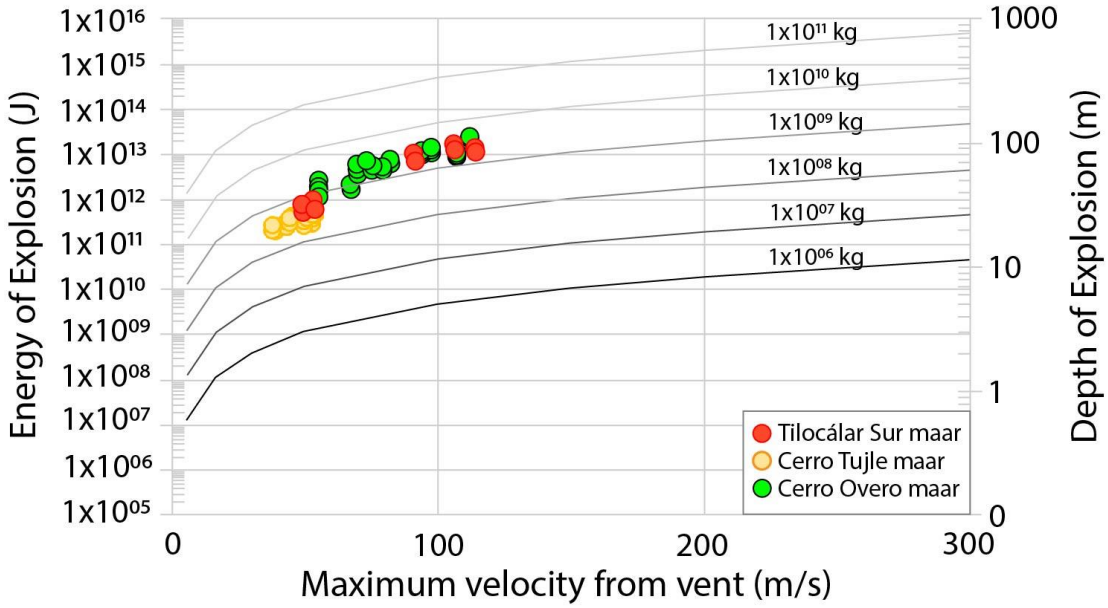

Figure 6. Plot of ejection velocity, the energy of the explosion, and the physical depth of explosion [93] for near-optimal scaled depth explosions for a range of ejected masses estimated from Valentine, et al. [92] (by gray lines). Data taken from Ureta, et al. [53], Ureta, et al. [50], and Ureta, et al. [54].

4.3. Eruption Styles

Based on the general morphological, morphometric, and sedimentary characteristics of the three scenarios in the study, the eruptive patterns are within the range of small maar volcanoes (300–600 m diameter) with respect to the crater diameter for maar volcanoes worldwide [3]. Although all the cases display a relatively small eruptive volume (Table 1), changes in the tephra deposit and bed characteristics, together with the type of xenoliths and lithics, suggest specific features in the fragmentation dynamic for each volcanic eruption.

Changes in eruptive style are typical amongst monogenetic volcanoes which typically shift from initial hydromagmatic phases with the deposition of surge deposit to a magmatic phase with the accumulation of scoria, spatter, and lava flows. This is characterized by the magma/water ratio and the explosive energy-melt fragmentation or mechanical energy [94,95] which are controlled by internal- (e.g., magma properties) and external- (e.g., environment) factors that determine the eruptive style and volcanic landforms [11,15,94,96]. In this context, the field observation, stratigraphic, morphological, petrographic, and geochemical characteristics of Tilocálar Sur, Cerro Tujle, and Cerro Overo volcanoes suggest a fast ascent rate of magma. Considering the groundwater availability of the local environment setting, the magma supply rate must be sufficiently high relative to the groundwater flux to overwhelm it and seal the conduit walls if the rising magma is to the surface without interacting with the water. In this context, through a relatively stagnant or slowly raised column of magma in the feeder conduit that does not exhibit an interaction initially with external water, generating a bursting of large gas pockets that is inferred to be responsible for Strombolian activity [97]. This type of magmatic fragmentation is dominated by the depressurization, transition from closed to open system [98] that characterizes a Strombolian activity [99,100]. Following this eruptive phase, the reduced eruptive volume and the stratigraphic sequence suggest a progressive decrease in the magma supply rate relative to the groundwater flux rate. Thus, when the magma supply rate is low and cannot overwhelm the available groundwater flow; the groundwater generates a collapse of the conduit wall allowing the entrance of groundwater and resulting contact with the magma, generating a phreatomagmatic eruption. This represents a self-driven violent interaction of magma and steam, known as molten fuel-coolant interaction (MFCI or FCI; [101,102]), which is sustained by thermal and hydrodynamic interaction between molten fuel (magma) and a coolant (water) (e.g., [81,103,104]).

Therefore, the deposits generated by Tilocálar Sur, Cerro Tujle, and Cerro Overo eruptions correspond to Strombolian to effusive and phreatomagmatic eruptive styles. Strombolian activity is characterized by fallout deposits, while the effusive stage is dominated by lava flow deposits. The deposits generated by a phreatomagmatic eruptive style are represented by surge deposit, ash and lapilli, juvenile breccia with lithic fragments, cauliflower and chilling textures, irregular and wide range of vesicles, and by a crater that cuts into the pre-eruptive landscape.

4.4. Magmatic Processes

The small-volume scale of monogenetic volcanoes enables preservation of the petrological features of the magmatic systems [13]. Juvenile material of monogenetic volcanoes is considered a "window to the mantle" allowing an insight into the processes that produce their magmas, (e.g., [105–110]), whereas the lithic content of these monogenetic systems could be considered as a "window to the crust and to the substrate" (e.g., [111–115]). In both senses, monogenetic volcanoes provide a unique opportunity to study the details of volcanic processes from the magmatic source to the surface.

Textural evidence for the Tilocálar Sur, Cerro Tujle, and Cerro Overo products is mainly characterized by fine-grained texture, skeletal morphologies of crystals (mainly of olivine phenocrysts; Figure 7a), high abundance of microlites (mainly plagioclase; Figure 7a), and the occurrence of sideromelane (Figure 7b). In addition, quartz xenocrysts with well-developed acicular clinopyroxene reaction coronas (Figure 7c) and fragments of country rocks (xenoliths) that display amphibole breakdown/reaction rim width with skeletal and sieve textures (Figure 7d) are present. Scoriaceous material (ash and lapilli) with cauliflower texture (Figure 7e), cooling crack, chilled margin (Figure 7f),

a wide range of vesicularity, breccias of juvenile material (Figure 7g), and impact of ballistically transported fragments (Figure 7h,i) were identified. These textural features correspond mainly to disequilibrium textures and indicate decompression, rapid cooling, and a relatively high magma ascent rate (e.g., [116–118]). On the other hand, the survival of quartz xenocrysts and country rocks fragments suggest a relatively short contact time of magma–country rock interaction, indicating a low degree of assimilation and any significant pausing of the magma within the CVZ thick crust (e.g., [108,109,119]). In addition, the occurrence of amphibole breakdown/reaction rim width with skeletal and sieve textures within the xenoliths suggest that a fine-scale magma mixing/mingling would have taken place during the magma ascent in the shallow crust at depths of 4–8 km and temperatures of 880–920 °C [120–122] which is concordant with the shallow magma reservoirs reported and suggested for the Altiplano-Puna area [67,123–125].

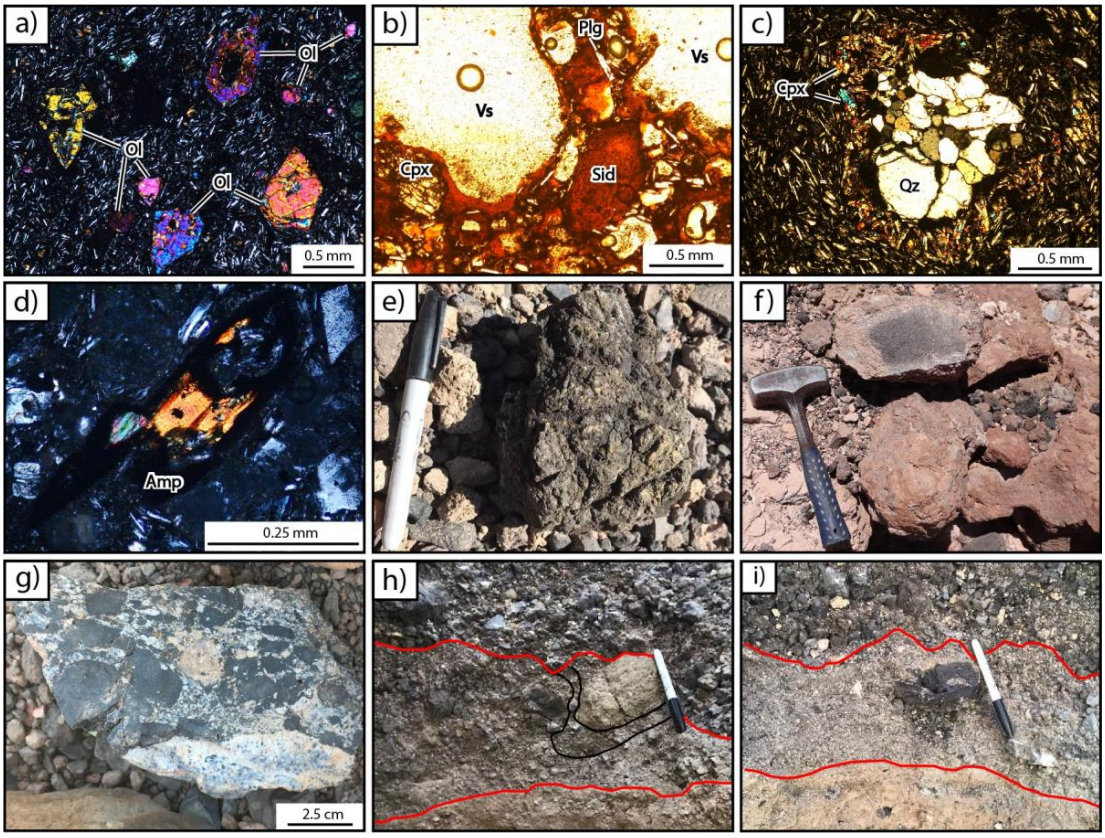

Figure 7. (**a**) Skeletal and sieve textures of olivine (Ol) phenocrysts from Cerro Overo maar (taken from [54]). (**b**) Orange-red sideromelane (Sid) associated with irregular vesicles (Vs), plagioclases (Plg), and clinopyroxenes (Cpx) from Tilocálar Sur maar (documented in detail in [53]). (**c**) Quartz (Qz) xenocrysts with well-developed acicular clinopyroxene (Cpx) reaction coronas from Tilocálar Sur maar (documented in detail in [53]). (**d**) Amphibole (Amp) breakdown/reaction rim width with skeletal and sieve textures from Cerro Tujle maar (documented in detail in [50]). (**e**) Scoria with cauliflower texture from Cerro Overo maar (taken from [54]). (**f**) Scoria with chilled margin from Tilocálar Sur maar (documented in detail in [53]). (**g**) Breccia of juvenile material from Cerro Tujle maar (documented in detail in [50]). (**h**,**i**) Impact of a ballistically transported fragment from Cerro Overo maar (documented in detail in [54]).

Geochemically, Tilocálar Sur maar, Cerro Tujle, and Cerro Overo products correspond to basaltic andesite to andesite (Figure 8a), calc-alkaline, and high-K calc-alkaline magmas (Figure 8b), with a relatively high concentration of incompatible trace elements, as enrichments of large-ion lithophile element (LILE) compared with high field strength elements (HFSE) (Figure 8c,d), and Sr isotope ratio content similar to the evolved felsic magmas of the Altiplano-Puna Volcanic Complex.

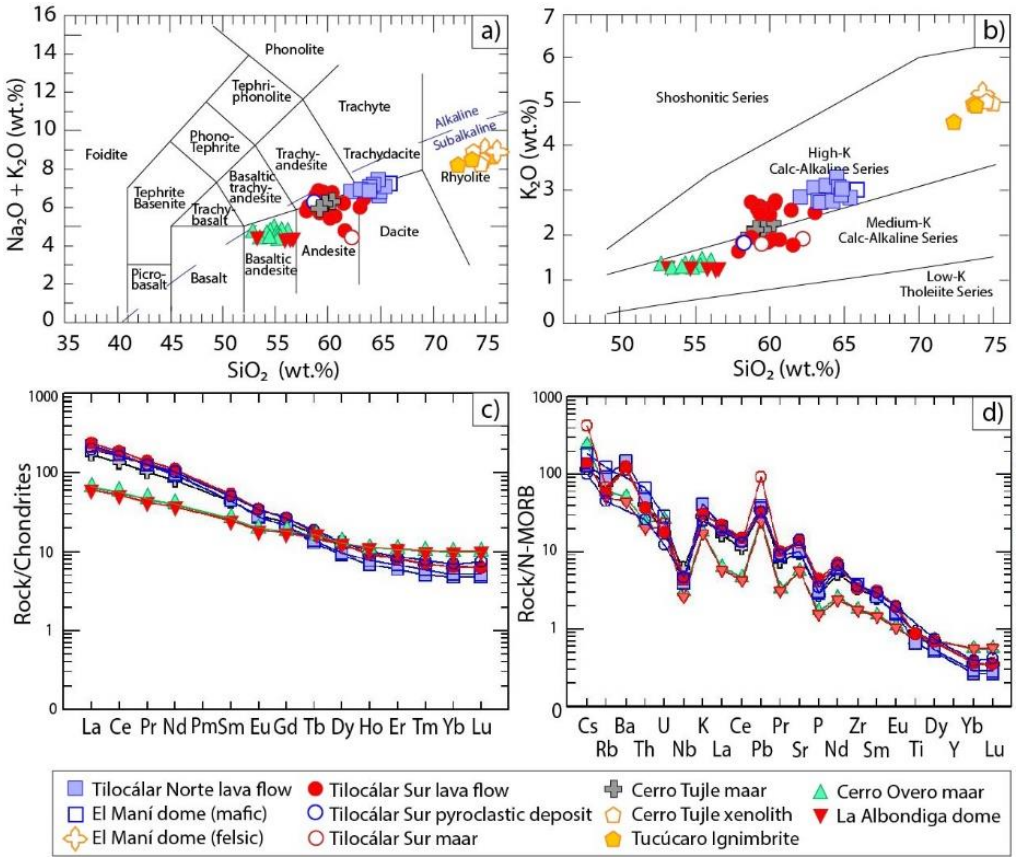

Figure 8. (**a**) TAS diagram (after [126]). (**b**) Alkali silica diagram [127]. (**c**,**d**) Multi-element diagrams, Chondrite and N-MORB, respectively (normalized values from [128]). Data taken from Ureta, et al. [53], Ureta, et al. [50], and Ureta, et al. [54].

Overall, all the samples display mixing processes that are evidenced in the absence of linear trends on variation diagrams. Besides, a regular trend of depletion in CaO, FeO, Cr, and Ni with decreasing MgO content suggests fractional crystallization (FC) processes consistent with the olivine ± spinel and clinopyroxene phenocrysts observed in the samples rocks (Figure 9a–c). These magmatic processes are expected in CVZ (e.g., [67,129–131]), considering the mafic nature of these magmas that are mantle-derived and have crossed a thick crust (~70 km depth) during their ascent to the surface. Despite this, all the products show a degree of crustal contamination, which is low but in the same range as magma stored in the crust during prolonged times at polygenetic volcanoes of the CVZ (Figure 9d).

Tilocálar Sur maar and the other monogenetic volcanoes of the Tilocálar monogenetic volcanic field [53] together with the Cerro Tujle maar evidenced deep assimilation [50]. In contrast, Cerro Overo maar [54] shows shallow assimilation like xenoliths from Cerro Tujle and the felsic part of the mingling of the El Maní dome at Tilocálar monogenetic volcanic field [53]. These characteristics are consistent with a fast ascent rate of the magma, without any prolonged pausing of the magma on route to the surface, and with the high content of xenoliths found mainly in Cerro Tujle maar with respect to the other maars in the study. These processes can explain the preservation of the mafic composition; nevertheless, they cannot fully explain the relatively high concentration of incompatible trace elements (LILE) and Sr isotope ratio contents because the FC was minor and the assimilation was selective, suggesting assimilation during a turbulent ascent process (ATA; [132]). ATA process produces a high assimilation/crystallization ratio during a relatively short time of magma–country rock interaction due to selective contamination at several depths and with crustal components [132–134]. Figure 9e,f shows a reverse isotopic content of decreasing Sr isotope ratio values during differentiation, and a variable range of Nd isotope ratio with a relative constant behavior of Nd, respectively. This magmatic

process is consistent with fine-grained textures, skeletal textures, xenoliths, and quartz xenocrysts found in the rock samples. ATA process has been suggested for Cerro Overo maar [54] and other centers in the Altiplano-Puna Volcanic Complex (e.g., [108,109,135–137]). This assimilation during the turbulent ascent process cannot be strongly supported for Cerro Tujle maar, Tilocálar Sur maar, and the other volcanoes of the Tilocálar monogenetic field due to the little amount of isotopic data available. Nevertheless, based on the textural evidence and chemical contents of trace elements, an ATA process for Cerro Tujle and Tilocálar monogenetic volcanic field could also be suggested.

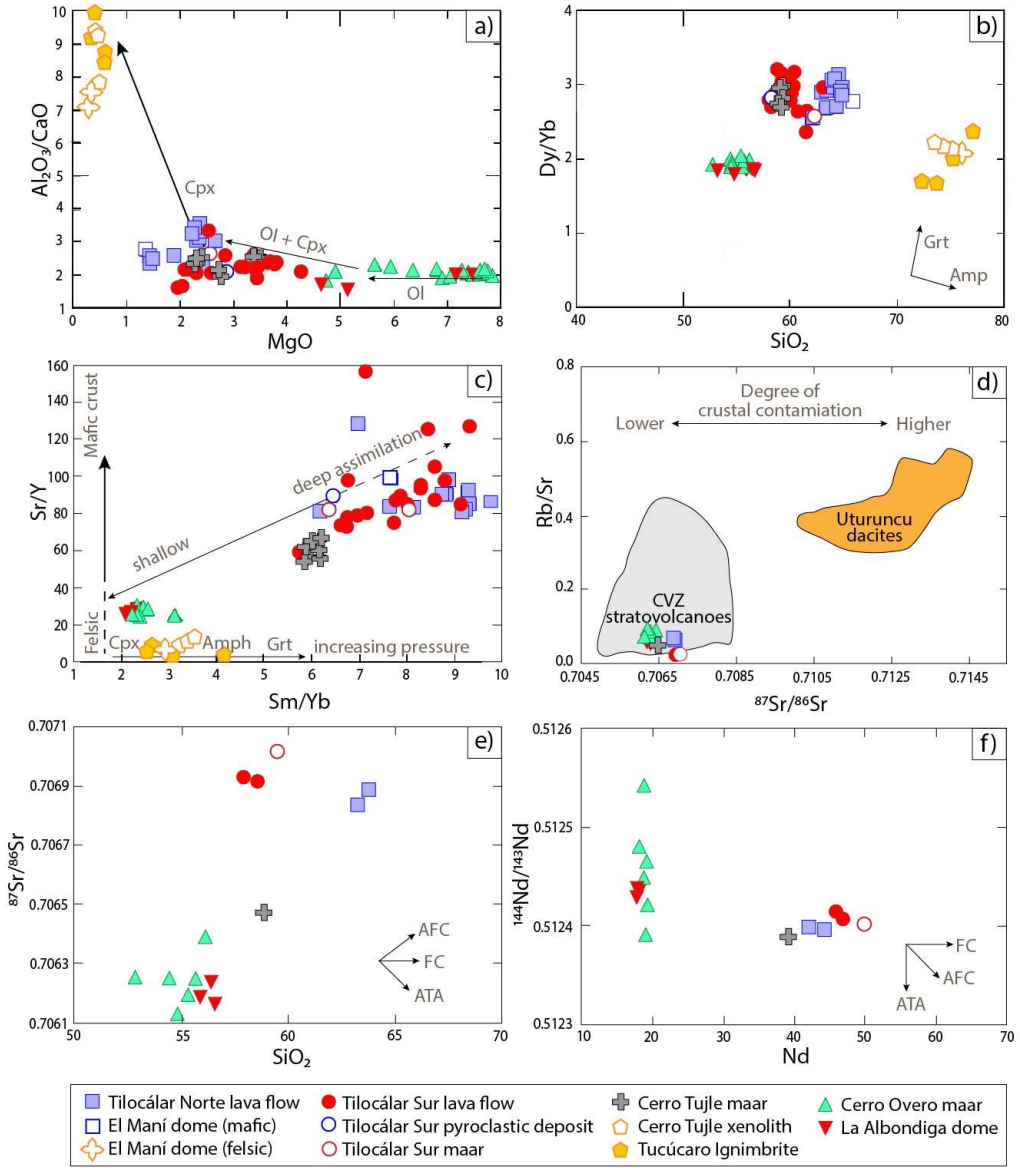

Figure 9. Diagrams showing (**a**) MgO (wt.%) vs. Al_2O_3/CaO, (**b**) Dy/Yb ratios vs. SiO_2 (wt.%), (**c**) Sm/Yb vs. Sr/Y ratios, (**d**) $^{87}Sr/^{86}Sr$ vs. Rb/Sr ratios, (**e**) $^{87}Sr/^{86}Sr$ vs. SiO_2 (wt.%), (**f**) $^{143}Nd/^{144}Nd$ vs. Nd (ppm). Data taken from Ureta, et al. [53], Ureta, et al. [50], and Ureta, et al. [54]. Arrows of differentiation trends after Mamani, et al. [66]. The diagram in (**d**) was modified from Taussi, et al. [138]. The values of both Rb/Sr and $^{87}Sr/^{86}Sr$ increase with an increasing degree of interaction with the partially molten Altiplano-Puna Magma Body. Grey and orange fields represent the Central Volcanic Zone (CVZ) of the Andes stratovolcano values from Mamani, et al. [66] and Uturruncu dacites from Michelfelder, et al. [139], respectively.

4.5. Proposed Model

Lorenz [9] and Valentine and White [6] have proposed a model for diatreme growths, which explains the presence of deep-seated country-rock lithics in tephra deposits formed by many phreatomagmatic explosions. Nevertheless, these proposed mechanisms for diatreme growth differ due to e.g., depression of the diatreme in the water table in some cases, the numbers and intensity of explosions, and the depth and the origin of the deep-seated country rock lithics present in ejecta ring deposits [6]. Following the strengths of both models and based on the main characteristics of Tilocálar Sur, Cerro Tujle, and Cerro Overo maar volcanoes, this work presents a set of features to help identify areas where maar volcanoes (phreatomagmatic eruptions) can potentially developed.

The three scenarios (Figure 9) studied are located at a high altitude environment of the Altiplano-Puna Plateau which, after the Tibetan Plateau, is the second-largest orogenic plateau in the world and which is characterized by key features that permit and favor the growth mechanisms for maar formations, namely:

i. A compressive tectonic setting, which generates folding systems represented by ridges structures forming a planar pathway at a shallow depth being auspicious for reservoirs (e.g., [75]) as groundwater tables. This tectonic setting generates the appropriate structural conditions to favor and form the space for groundwater channels that can host lenses of water bodies.
ii. Groundwater recharge, although the Altiplano-Puna area is an arid environment, the recharge of groundwater systems is favored by the snowmelt contribution which is seasonal (e.g., austral winter months) and greater at elevations above 4700 m a.s.l. [87,88].
iii. The lithological setting, characterized by alluvial sediments of variable thickness, overlying fractured andesitic lavas, large ignimbritic deposits, and erosional or weathered interlayered volcanic deposits (e.g., [44,48]). The large ignimbrite sheets are commonly extensively welded and/or hydrothermally altered, displaying layers of low permeability and permeable volcanic-derived sediments [88]. They form a regional groundwater flow base dipping gently away from their respective sources that do not follow the present-day topography marked by complex medium-volume stratovolcanic cone caps [85,86]. Besides, these extensive Pleistocene ignimbrite sheets are relatively shallow beneath cover beds, especially in areas between major stratovolcanoes. In those inter-cone areas, they are covered by debris fans that commonly shed run-off towards local lowlands that functioned as large but shallow lakes in pluvial periods (today, they are salars).
iv. The presence of aquifer and/or endorheic basins (e.g., lakes or salars), in the Altiplano area, which demonstrates the occurrence of groundwater flows among closed basins, which provide the hydraulic connection between groundwater levels (e.g., [85]).
v. A period of stress relaxation, although the Altiplano-Puna is dominated by a compressional tectonic setting, monogenetic volcanism has been associated with local extension permitting the magma to ascend to the surface (e.g., [140]).

Considering the characteristics mentioned above (Figure 10a), it is possible to identify places where phreatomagmatic eruptions could occur, depending on if the magma flux rate is outmatched by the groundwater table flux during the ascent from the source to the surface i.e., Tilocálar Sur, Cerro Tujle, and Cerro Overo maar volcanoes. The cooling down of the magma against the initially cold surrounding host rock may line the conduit walls with a viscous melt that tends to seal off the groundwater as the magma rises and emerges to the surface [23,25], generating a magmatic explosive or effusive activity as pyroclastic deposit or lava effusion, respectively (Figure 10b–d; e.g., [29]).

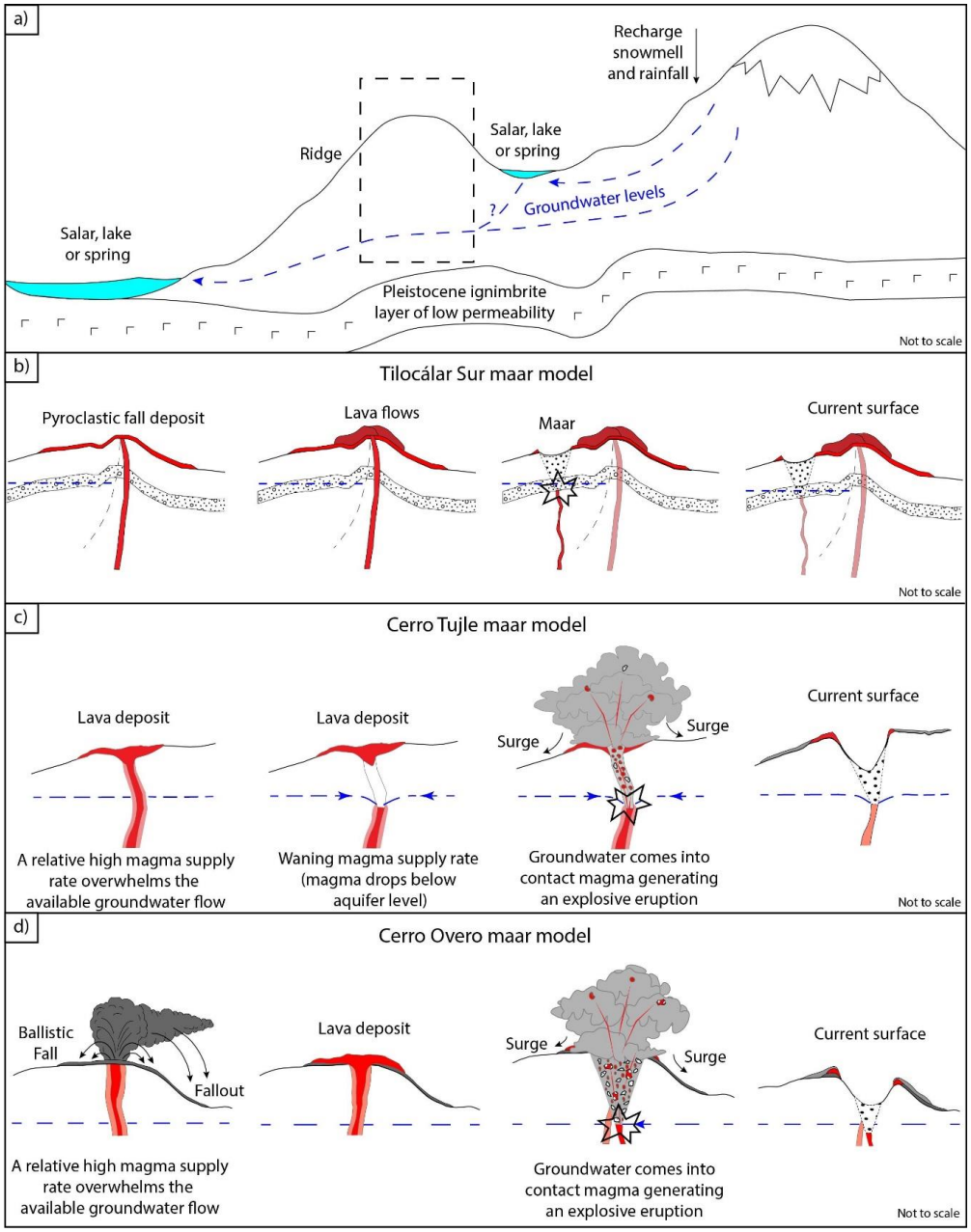

Figure 10. Proposed model of the mechanism of maar development. (**a**) Lithological and hydrogeological factors that favor phreatomagmatism in northern Chile (modified after [87,88]). The inserted box corresponds to Figure 10b–d, respectively. (**b–d**) Mechanisms of magma–water interaction for maars in northern Chile (model based on [50,53,54]).

In this context, during the late stage of the magmatic eruption, a gradual decrease in the mass eruption rate is generated which produces an inward collapse of the wall of the conduit followed by a blockage of the opening. This process occurs by a gradual drawback of the magma within the conduit below the groundwater table level which the lava had drained, generating lithostatic pressure and a sudden entry of groundwater into the volcanic conduit allowing the magma–water interaction (e.g., [22–25,28]). On the other hand, if the magma flux is outmatched by the groundwater flux, the groundwater comes into contact with magma generating a phreatomagmatic eruption (Figure 10c). Both mechanisms of magma–water interaction are suggested for the Tilocálar Sur maar, Cerro Tujle maar, and Cerro Overo maar (Figure 10).

Based on the interplay between the internal- and external- factors previously mentioned, it is possible to suggest that areas dominated by a basement of ignimbrites, presence of lakes or salars, and ridge structures are auspicious for phreatomagmatic eruptions which could be associated with non-phreatomagmatic tephra interlayered as magmatic explosive and/or magmatic effusive deposits. Nevertheless, if the location of the vent is closer to lakes or salars the magma–water ratios can increase, generating Surtseyan eruptions building tuff rings or tuff cones [94]. This set of features deployed to recognize the location of growth and fragmentation of phreatomagmatic eruptions that form maar volcanoes is supported by the maars reported by Filipovich, et al. [141] in the Pasto Ventura monogenetic volcanic field, Puna Austral (Figure 11). Pasto Ventura's maars are located on the ridges (compressive tectonic setting), associated with water-saturated areas, endorheic basins such as lakes, groundwater recharge related to stratovolcanoes with snow, and rainfall by the Altiplanic winter (Figure 11). Therefore, the key features presented in this work could be applied in other areas of the Altiplano-Puna where the occurrence of monogenetic volcanism has taken place as a cluster (e.g., Pasto Ventura; Figure 11) or as isolated events (e.g., Cerro Overo; Figure 11).

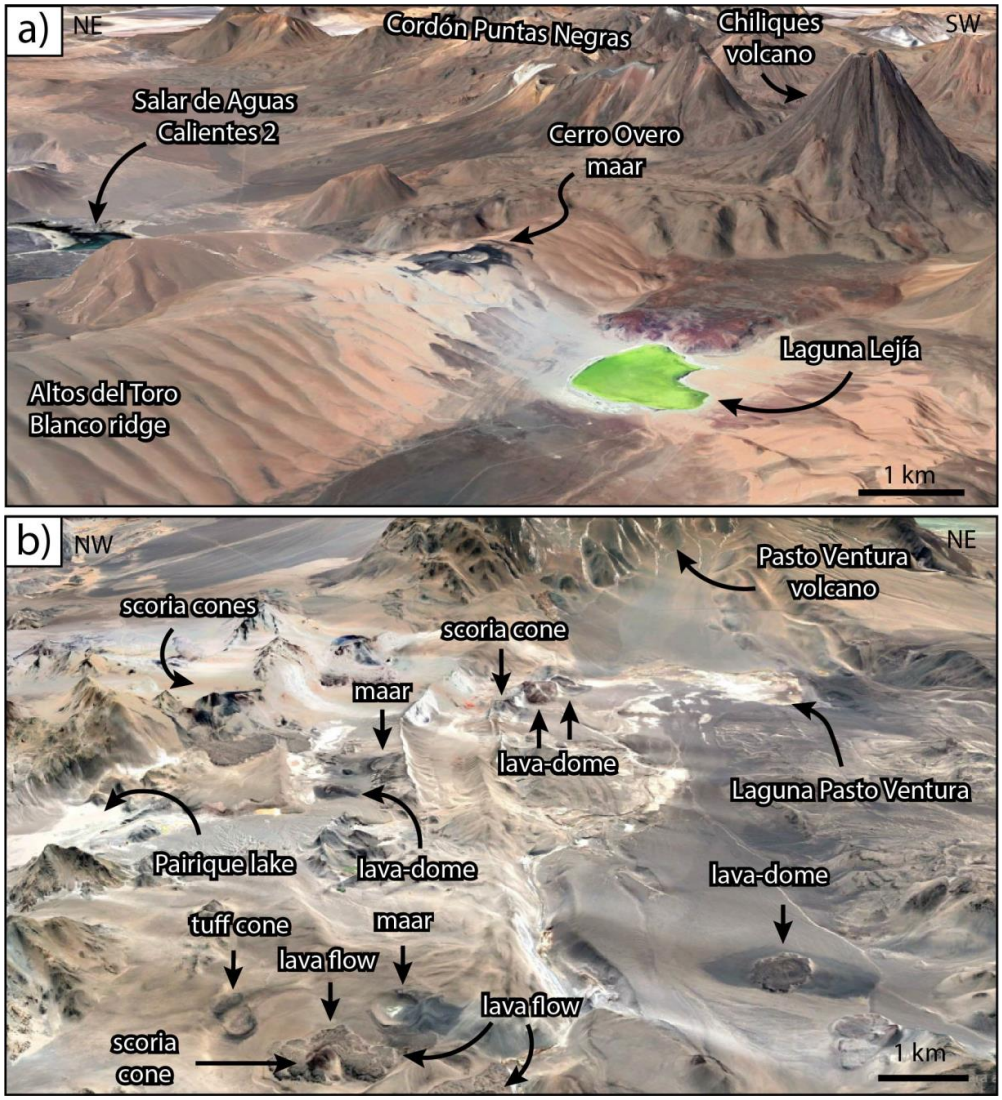

Figure 11. Examples of scenarios that permit and favor the growth mechanisms for maar formations are characterized by the presence of ridge structures and flux of groundwater evidenced by the occurrence of lakes. (**a**) Cerro Overo area, northern Chile. (**b**) Pasto Ventura monogenetic volcanic field, Puna Argentina. Satellite images are taken from Google Earth™.

This transition of different eruption processes is recorded and evidenced in Strombolian eruptions as pyroclastic deposits and lava effusion to phreatomagmatic eruption as surge deposits and could take place in the temporal transitions at a single vent (e.g., Cerro Tujle maar) or at different vents within the same maar system (e.g., Tilocálar Sur maar and Cerro Overo maar). This is consistent with the model of maar growth suggested by Valentine and White [6], implying transitions into and out of phreatomagmatic activity during a maar-forming eruption reflecting variations of magma flux, inhomogeneous water distribution, and other influences on explosion initiation.

5. Concluding Remarks

Maar volcanoes in northern Chile are characterized by preserved craters that cut into the pre-eruptive landscape which display a pyroclastic deposit (tephra ring), continuous deposit sequences of lavas and scorias (short timescale), lapilli fragments and breccias with juvenile material, single volcanic structure, host rock mainly composed of ignimbrites with the permeability required to confining water layers, simple conduit system (plumbing), a small volume of erupted magma (<1 km^3), and various magma compositions (from basaltic andesite to andesite). The magmas that formed these maars correspond to mantle-derived magmas that during their ascent from the source to the surface, have experienced various magmatic processes such as mixing, FC, ATA, and magma–water interaction. However, despite the absence of naked eye evidence of a typical magma–water interaction such as thick surge levels, cross-bedded tuffs, abundant clasts emplaced from ballistic trajectories, and the other features described in the literature [8,15,30,31,142], at least two eruptive stages for each maar in the study are suggested in this work. The first stage is an ephemeral magmatic explosive to magmatic effusive condition where the magma may ascend and feed intrusions without interacting with water in the conduit and reaches the surface to erupt as a pyroclastic and/or lava deposit. The second stage is a hydromagmatic explosive condition dominated by magma–water interaction between 25 m to 115 m depth, along feeder dike, which forms a crater, tephra ring (such as ash and lapilli fragments that present a great range of vesicularity, cooling cracks, cauliflower textures, chilled margins, and breccia fragments with juvenile material and lithic clasts), and domains of brecciated country rock in the subsurface.

In this context, the phreatomagmatic eruptions in northern Chile depend and are favored mainly by a compressive tectonic setting that favors and forms the space for ground-water channels that can host lenses of water bodies (e.g., folds or ridges), the lithological setting, the groundwater recharge and discharge, the presence of aquifer and/or endorheic basins (e.g., lakes or salars), the period of stress relaxation, and by a magma flux lower than the groundwater flux. This set of features that favor phreatomagmatic eruptions forming maar volcanoes could be applied to identify possible sites worldwide where the magma–water interaction eruption could occur. This could be useful for the prediction of hydromagmatic volcanic eruptions and for mitigating the impact of volcanic hazard for the inhabitants of such locations. However, geochemical data of the eruptive sequence of juvenile products, hydrological studies, and magnetic and geophysical measurements are necessary for further constraints and in order to obtain a better understanding of the prediction of the emplacement location of maar volcanoes, especially if these key features recur in other maars at other geological settings around the world.

Author Contributions: Conceptualization, G.U. and K.N.; methodology, G.U.; software, G.U.; validation, G.U., K.N., F.A. and R.G.; formal analysis, G.U., K.N., F.A. and R.G.; investigation, G.U., K.N. and F.A.; resources, G.U. and F.A.; data curation, G.U., K.N. and F.A.; writing—original draft preparation, G.U., K.N. and F.A.; writing—review and editing, G.U., K.N., F.A. and R.G.; visualization, G.U.; supervision, K.N. and F.A.; project administration, G.U. and F.A.; funding acquisition, G.U. and F.A. All authors have read and agreed to the published version of the manuscript.

Funding: This research is part of a G.U. Ph.D. thesis, which is funded by the CONICYT-PCHA Doctorado Nacional 2016-21161286 fellowship and supported by the Universidad Católica del Norte. This study is emerged and funded by CONICYT-PAI MEC 2017-80170048 (titled "*Fortalecimiento del área de volcanismo en el Departamento de Ciencias Geológicas*"), and the Antofagasta Regional Government, FIC-R project, code BIP Nº30488832-0 (titled "*Mitigación del riesgo asociado a procesos volcánicos en la Región de Antofagasta*"); based on the Memorandum of Understanding of Research Cooperation between Universidad Católica del Norte and Massey University.

Acknowledgments: The authors wish to thank Mary T. Lavin-Zimmer for editing of the English language. Besides, the authors wish to thank all members of the Núcleo de Investigación en Riesgo Volcánico Ckelar Volcanes team for fruitful discussions.

Conflicts of Interest: The authors declare no conflict of interest. The funders had no role in the design of the study; in the collection, analyses, or interpretation of data; in the writing of the manuscript, or in the decision to publish the results.

References

1. Vespermann, D.; Schmincke, H.-U. Scoria cones and tuff rings. In *Encyclopedia of Volcanoes*; Sigurdsson, H., Houghton, B., McNutt, S., Rymer, H., Stix, J., Eds.; Academic Press: Cambridge, MA, USA, 2000; pp. 683–694.
2. Lorenz, V. Syn- and posteruptive hazards of maar–diatreme volcanoes. *J. Volcanol. Geotherm. Res.* **2007**, *159*, 285–312. [CrossRef]
3. Graettinger, A.H. Trends in maar crater size and shape using the global Maar Volcano Location and Shape (MaarVLS) database. *J. Volcanol. Geotherm. Res.* **2018**, *357*, 1–13. [CrossRef]
4. Lorenz, V. On the formation of maars. *Bull. Volcanol.* **1973**, *37*, 183–204. [CrossRef]
5. White, J.D.L.; Ross, P.S. Maar-diatreme volcanoes: A review. *J. Volcanol. Geotherm. Res.* **2011**, *201*, 1–29. [CrossRef]
6. Valentine, G.A.; White, J.D.L. Revised conceptual model for maar-diatremes: Subsurface processes, energetics, and eruptive products. *Geology* **2012**, *40*, 1111–1114. [CrossRef]
7. Ross, P.-S.; Carrasco Núñez, G.; Hayman, P. Felsic maar-diatreme volcanoes: A review. *Bull. Volcanol.* **2017**, *79*. [CrossRef]
8. Lorenz, V. Maars and diatremes of phreatomagmatic origin; a review. *S. Afr. J. Geol.* **1985**, *88*, 459–470.
9. Lorenz, V. On the growth of maars and diatremes and its relevance to the formation of tuff rings. *Bull. Volcanol.* **1986**, *48*, 265–274. [CrossRef]
10. Lorenz, V.; Suhr, P.; Suhr, S. Phreatomagmatic maar-diatreme volcanoes and their incremental growth: A model. *Geol. Soc. Lond. Spec. Publ.* **2016**, *446*, 29–59. [CrossRef]
11. Kereszturi, G.; Németh, K. Monogenetic Basaltic Volcanoes: Genetic Classification, Growth, Geomorphology and Degradation. In *Updates in Volcanology-New Advances in Understanding Volcanic Systems*; Németh, K., Ed.; Intech Open: London, UK, 2012; Chapter 1; pp. 3–88.
12. Németh, K.; Kereszturi, G. Monogenetic volcanism: Personal views and discussion. *Int. J. Earth Sci.* **2015**, *104*, 2131–2146. [CrossRef]
13. Smith, I.E.M.; Németh, K. Source to surface model of monogenetic volcanism: A critical review. In *Monogenetic Volcanism*; Németh, K., Carrasco-Núñez, G., Aranda-Gómez, J.J., Smith, I.E.M., Eds.; Geological Society: London, UK, 2017; Volume 446, Chapter 1; pp. 1–28.
14. Németh, K. Monogenetic volcanic fields: Origin, sedimentary record, and relationship with polygenetic volcanism. In *What Is a Volcano?* Canon-Tapia, E., Szakacs, A., Eds.; Geological Society of America: Boulder, CO, USA, 2010; Volume 470, pp. 43–66.
15. Németh, K.; Kósik, S. Review of Explosive Hydrovolcanism. *Geosciences* **2020**, *10*, 44. [CrossRef]
16. Németh, K.; Kósik, S. The role of hydrovolcanism in the formation of the Cenozoic monogenetic volcanic fields of Zealandia. *N. Z. J. Geol. Geophys.* **2020**, 1–26. [CrossRef]
17. Valentine, G.A.; White, J.D.L.; Ross, P.-S.; Amin, J.; Taddeucci, J.; Sonder, I.; Johnson, P.J. Experimental craters formed by single and multiple buried explosions and implications for volcanic craters with emphasis on maars. *Geophys. Res. Lett.* **2012**, *39*. [CrossRef]
18. Valentine, G.A.; White, J.D.L.; Ross, P.-S.; Graettinger, A.H.; Sonder, I. Updates to Concepts on Phreatomagmatic Maar-Diatremes and Their Pyroclastic Deposits. *Front. Earth Sci.* **2017**, *5*. [CrossRef]
19. Bishop, M.A. A generic classification for the morphological and spatial complexity of volcanic (and other) landforms. *Geomorphology* **2009**, *111*, 104–109. [CrossRef]
20. Kósik, S.; Németh, K.; Lexa, J.; Procter, J.N. Understanding the evolution of a small-volume silicic fissure eruption: Puketerata Volcanic Complex, Taupo Volcanic Zone, New Zealand. *J. Volcanol. Geotherm. Res.* **2019**, *383*, 28–46. [CrossRef]
21. Murcia, H.; Németh, K.; El-Masry, N.N.; Lindsay, J.M.; Moufti, M.R.H.; Wameyo, P.; Cronin, S.J.; Smith, I.E.M.; Kereszturi, G. The Al-Du'aythah volcanic cones, Al-Madinah City: Implications for volcanic hazards in northern Harrat Rahat, Kingdom of Saudi Arabia. *Bull. Volcanol.* **2015**, *77*, 54. [CrossRef]
22. Gutmann, J.T. Geology of Crater Elegante, Sonora, Mexico. *Gsa Bull.* **1976**, *87*, 1718–1729. [CrossRef]

23. Gutmann, J.T. Strombolian and effusive activity as precursors to phreatomagmatism: Eruptive sequence at maars of the Pinacate volcanic field, Sonora, Mexico. *J. Volcanol. Geotherm. Res.* **2002**, *113*, 345–356. [CrossRef]
24. Decker, R.W.; Christiansen, R.L. *Explosive Eruptions of Kilauea Volcano, Hawaii*; National Academy Press: Washington, DC, USA, 1984; p. 12.
25. Swanson, D.; Fiske, D.; Rose, T.; Houghton, B.; Mastin, L. Kīlauea—An Explosive Volcano in Hawai 'i. *U. S. Geol. Surv.* **2011**, *4*. [CrossRef]
26. Houghton, B.; White, J.D.L.; Van Eaton, A.R. Phreatomagmatic and Related Eruption Styles. In *The Encyclopedia of Volcanoes*, 2nd ed.; Sigurdsson, H., Houghton, B., McNutt, S.R., Rymer, H., Stix, J., Eds.; Academic Press: Cambridge, MA, USA, 2015; pp. 537–552.
27. Németh, K. The morphology and origin of wide craters at Al Haruj al Abyad, Libya: Maars and phreatomagmatism in a large intracontinental flood lava field? *Z. Für Geomorphol.* **2004**, *48*, 417–439.
28. Báez, W.; Carrasco Nuñez, G.; Giordano, G.; Viramonte, J.G.; Chiodi, A. Polycyclic scoria cones of the Antofagasta de la Sierra basin, Southern Puna plateau, Argentina. In *Monogenetic Volcanism*; Németh, K., Carrasco-Núñez, G., Aranda-Gómez, J.J., Smith, I.E.M., Eds.; Geological Society: London, UK, 2017; Volume 446, Chapter 311; pp. 311–336.
29. Sweeney, M.R.; Grosso, Z.S.; Valentine, G.A. Topographic controls on a phreatomagmatic maar-diatreme eruption: Field and numerical results from the Holocene Dotsero volcano (Colorado, USA). *Bull. Volcanol.* **2018**, *80*, 78. [CrossRef]
30. White, J.D.L.; Valentine, G.A. Magmatic versus phreatomagmatic fragmentation: Absence of evidence is not evidence of absence. *Geosphere* **2016**, *12*, 1478–1488. [CrossRef]
31. Latutrie, B.; Ross, P.-S. Phreatomagmatic vs magmatic eruptive styles in maar-diatremes: A case study at Twin Peaks, Hopi Buttes volcanic field, Navajo Nation, Arizona. *Bull. Volcanol.* **2020**, *82*, 28. [CrossRef]
32. Lorenz, V. Maar-diatreme volcanoes, their formation, and their setting in hard-rock or soft-rock environments. *Geolines* **2003**, *15*, 72–83.
33. Ureta, G.; Németh, K.; Aguilera, F.; Vilches, M.; Aguilera, M.; Torres, I.; Sepúlveda, J.P.; Scheinost, A.; González, R. An overview of the mafic and felsic monogenetic Neogene to Quaternary volcanism in the Central Andes, northern Chile (18–28°Lat.S). In *Volcanoes-Updates in Volcanology*; Németh, K., Ed.; IntechOpen: London, UK, 2020. [CrossRef]
34. Yokoyama, I. Eruption patterns of parasitic volcanoes. *Ann. Geophys.* **2015**, *58*, 0327.
35. González-Ferrán, O. *Volcanes de Chile*; Instituto Geográfico Militar: Santiago, Chile, 1995; p. 640.
36. De Silva, S.L.; Francis, P.W. *Volcanoes of the Central Andes*; Springer: Berlin/Heidelberg, Germany, 1991; p. 216.
37. Tornos, F.; Velasco, F.; Hanchar, J.M. The Magmatic to Magmatic-Hydrothermal Evolution of the El Laco Deposit (Chile) and Its Implications for the Genesis of Magnetite-Apatite Deposits. *Econ. Geol.* **2017**, *112*, 1595–1628. [CrossRef]
38. Cornejo, P.N.; Naranjo, J.A. Azufrera Juan de la Vega: Un maar de origen freatomagmático, Andes del norte de Chile(25°52′ S). In Proceedings of the V Congreso Geológico de Chile, Santiago, Chile, 8–12 August 1988; pp. 209–227.
39. Gardeweg, M.; Clavero, J.; Mpodozis, C.; Pérez de Arce, C.; Villeneuve, M. El Macizo Tres Cruces: Un complejo volcánico longevo y potencialmente activo en la Alta Cordillera de Copiapó, Chile. In Proceedings of the IX Congreso Geológico Chileno, Puerto Varas, Chile, 31 July–4 August 2000; pp. 291–295.
40. Lienlaf, J. Volcanismo Freatomagmático del Mioceno Superior de los Andes Centrales del norte de Chile. Master's Thesis, Universidad de Chile, Santiago, Chile, 2019.
41. Kött, A.; Gaupp, R.; Wörner, G. Miocene to recent history of the western Altiplano in northern Chile revealed by lacustrine sediments of the Lauca basin (18°15′–18°40′ S/69°30′–69°05′ W). *Geol. Rundsch.* **1995**, *84*, 770–780. [CrossRef]
42. Francis, P.; de Silva, S.; Mouginis-Mark, P.; Self, S. *Twentieth Lunar and Planetary Science Conference*; LPI Contribution No. 1586; Lunar and Planetary Institute: Houston, TX, USA, 1989; Volume 20, pp. 307–308.
43. de Silva, S.L.; Self, S.; Francis, P.W. A new class of volcanic center from N. Chile? *EosTrans. Am. Geophys. Union* **1988**, *69*, 1491. [CrossRef]
44. Gardeweg, M.; Ramirez, C.F. Geological Map of Hoja Rio Zapaleri. II Region de Antofagasta. Escala 1: 250.000. 1985.
45. Self, S.; de Silva, S.L.; Cortés, J.A. Enigmatic clastogenic rhyolitic volcanism: The Corral de Coquena spatter ring, North Chile. *J. Volcanol. Geotherm. Res.* **2008**, *177*, 812–821. [CrossRef]

46. Gardeweg, M.; Ramírez, C.F. La Pacana caldera and the Atana Ignimbrite—A major ash-flow and resurgent caldera complex in the Andes of northern Chile. *Bull. Volcanol.* **1987**, *49*, 547–566. [CrossRef]
47. van Alderwerelt, B.M.E.d.R. Diverse Monogenetic Volcanism Across the Main Arc of the Central Andes, Northern Chile. Ph.D. Thesis, University of Iowa, Iowa City, IA, USA, 2017.
48. Ramírez, C.F.; Gardeweg, M.P. *Geological Map of Hoja Toconao, Región de Antofagasta*; Instituto Geografico Militar: Santiago, Chile, 1982; Volume 54.
49. Ureta, G. Evolución Geológica y Petrológica del Volcán Cerro Overo. Master's Thesis, Universidad Católica del Norte, Antofagasta, Chile, 2015.
50. Ureta, G.; Aguilera, F.; Németh, K.; Inostroza, M.; González, C.; Zimmer, M.; Menzies, A. Transition from small-volume ephemeral lava emission to explosive hydrovolcanism: The case of Cerro Tujle maar, northern Chile. *J. S. Am. Earth Sci.* **2020**, *104*, 102885. [CrossRef]
51. Gardeweg, M.; Ramirez, C.F. Geología de los volcanes del Callejón de Tilocálar, Cordillera de los Andes—Antofagasta. In Proceedings of the III Congreso Geológico Chileno, A111-A-123, Antofagasta, Chile, 4–14 November 1982.
52. Stearns, H.T.; Macdonald, G.A. *Geology and Ground-Water Resources of the Island of Hawaii*; Report No. 9; Honolulu Advertising: Honolulu, HI, USA, 1946; p. 363.
53. Ureta, G.; Németh, K.; Aguilera, F.; Kósik, S.; González, R.; Menzies, A.; González, C.; James, D. Evolution of a magmatic explosive/effusive to phreatomagmatic volcanic system: Birth of a monogenetic volcanic field, Tilocálar volcanoes, northern Chile. *J. Volcanol. Geotherm. Res.*. under review.
54. Ureta, G.N.K.; Aguilera, F.; Zimmer, M.; Menzies, A. A window of mantle-derived magmas within the Central Andes: A case study of shifting from magmatic to phreatomagmatic fragmentation at the Cerro Overo maar, northern Chile. *Bull. Volcanol.*. under review.
55. Thorpe, R.S.; Francis, P.W. Variations in andean andesite compositions and their petrogenetic significance. *Tectonophysics* **1979**, *57*, 53–70. [CrossRef]
56. Global Volcanism Program. *Volcanoes of the World*; v. 4.8.5; Smithsonian Institution: Washington DC, USA, 2013. [CrossRef]
57. Trumbull, R.B.; Riller, U.; Oncken, O.; Scheuber, E.; Munier, K.; Hongn, F. The Time-Space Distribution of Cenozoic Volcanism in the South-Central Andes: A New Data Compilation and Some Tectonic Implications. In *The Andes: Active Subduction Orogeny*; Oncken, O., Chong, G., Franz, G., Giese, P., Götze, H.-J., Ramos, V.A., Strecker, M.R., Wigger, P., Eds.; Springer: Berlin/Heidelberg, Germany, 2006; pp. 29–43.
58. Zandt, G.; Leidig, M.; Chmielowski, J.; Baumont, D.; Yuan, X. Seismic Detection and Characterization of the Altiplano-Puna Magma Body, Central Andes. *Pure Appl. Geophys.* **2003**, *160*, 789–807. [CrossRef]
59. de Silva, S.L. Altiplano-Puna volcanic complex of the central Andes. *Geology* **1989**, *17*, 1102–1106. [CrossRef]
60. Stern, C.R. Active Andean volcanism: Its geologic and tectonic setting. *Rev. Geológica De Chile* **2004**, *31*, 161–206. [CrossRef]
61. Thorpe, R.S. The Tectonic Setting of Active Andean Volcanism. In *Andean Magmatism: Chemical and Isotopic Constraints*; Harmon, R.S., Barreiro, B.A., Eds.; Birkhäuser: Boston, MA, USA, 1984; pp. 4–8.
62. Francis, P.W.; De Silva, S.L. Application of the Landsat Thematic Mapper to the identification of potentially active volcanoes in the central Andes. *Remote Sens. Environ.* **1989**, *28*, 245–255. [CrossRef]
63. Dorbath, C.; Paul, A.; Group, T.L.A. Tomography of the Andean crust and mantle at 20° S: First results of the Lithoscope experiment. *Phys. Earth Planet. Inter.* **1996**, *97*, 133–144. [CrossRef]
64. Somoza, R. Updated azca (Farallon)—South America relative motions during the last 40 My: Implications for mountain building in the central Andean region. *J. S. Am. Earth Sci.* **1998**, *11*, 211–215. [CrossRef]
65. Thorpe, R.S.; Francis, P.W.; O'Callaghan, L. Relative roles of source composition, fractional crystallization and crustal contamination in the petrogenesis of Andean volcanic rocks. *Philos. Trans. R. Soc. Lond. Ser. AMath. Phys. Sci.* **1984**, *310*, 675–692. [CrossRef]
66. Mamani, M.; Worner, G.; Sempere, T. Geochemical variations in igneous rocks of the Central Andean orocline (13 S to 18 S): Tracing crustal thickening and magma generation through time and space. *Geol. Soc. Am. Bull.* **2010**, *122*, 162–182. [CrossRef]
67. de Silva, S.L.; Kay, S.M. Turning up the Heat: High-Flux Magmatism in the Central Andes. *Elements* **2018**, *14*, 245–250. [CrossRef]
68. Allmendinger, R.W. Tectonic development, southeastern border of the Puna Plateau, northwestern Argentine Andes. *Geol. Soc. Am. Bull.* **1986**, *97*. [CrossRef]

69. James, D.E. Andean crustal and upper mantle structure. *J. Geophys. Res.* **1971**, *76*, 3246–3271. [CrossRef]
70. Yuan, X.; Sobolev, S.V.; Kind, R. Moho topography in the central Andes and its geodynamic implications. *Earth Planet. Sci. Lett.* **2002**, *199*, 389–402. [CrossRef]
71. Guzmán, S.; Grosse, P.; Montero-López, C.; Hongn, F.; Pilger, R.; Petrinovic, I.; Seggiaro, R.; Aramayo, A. Spatial–temporal distribution of explosive volcanism in the 25–28° S segment of the Andean Central Volcanic Zone. *Tectonophysics* **2014**, *636*, 170–189. [CrossRef]
72. Rissmann, C.; Leybourne, M.; Benn, C.; Christenson, B. The origin of solutes within the groundwaters of a high Andean aquifer. *Chem. Geol.* **2015**, *396*, 164–181. [CrossRef]
73. Kuhn, D. Fold and thrust belt structures and strike-slip faulting at the SE margin of the Salar de Atacama basin, Chilean Andes. *Tectonics* **2002**, *21*, 8-1–8-17. [CrossRef]
74. Aron, F. Arquitectura y Estilo de la Deformación Compresiva Neógena del Borde Sur-Oriental del Salar de Atacama, Norte de Chile (23 30′sur): Su relación con el Volcanismo Pliocuaternario de los Andes Centrales. Master's Thesis, Universidad Católica del Norte, Antofagasta, Chile, 2008.
75. González, G.; Cembrano, J.; Aron, F.; Veloso, E.E.; Shyu, J.B.H. Coeval compressional deformation and volcanism in the central Andes, case studies from northern Chile (23° S–24° S). *Tectonics* **2009**, *28*. [CrossRef]
76. O'Callaghan, L.J.; Francis, P.W. Volcanological and petrological evolution of San Pedro volcano, Provincia EI Loa, North Chile. *J. Geol. Soc.* **1986**, *143*, 275–286. [CrossRef]
77. Berghuijs, J.F.; Mattsson, H.B. Magma ascent, fragmentation and depositional characteristics of "dry" maar volcanoes: Similarities with vent-facies kimberlite deposits. *J. Volcanol. Geotherm. Res.* **2013**, *252*, 53–72. [CrossRef]
78. Jordan, S.C.; Cas, R.A.F.; Hayman, P.C. The origin of a large (>3km) maar volcano by coalescence of multiple shallow craters: Lake Purrumbete maar, southeastern Australia. *J. Volcanol. Geotherm. Res.* **2013**, *254*, 5–22. [CrossRef]
79. Lierenfeld, M.B.; Mattsson, H.B. Geochemistry and eruptive behaviour of the Finca la Nava maar volcano (Campo de Calatrava, south-central Spain). *Int. J. Earth Sci.* **2015**, *104*, 1795–1817. [CrossRef]
80. Zimanowski, B.; Büttner, R.; Lorenz, V.; Häfele, H.-G. Fragmentation of basaltic melt in the course of explosive volcanism. *J. Geophys. Res. Solid Earth* **1997**, *102*, 803–814. [CrossRef]
81. Zimanowski, B.; Fröhlich, G.; Lorenz, V. Quantitative experiments on phreatomagmatic explosions. *J. Volcanol. Geotherm. Res.* **1991**, *48*, 341–358. [CrossRef]
82. Risacher, F.; Alonso, H.; Salazar, C. *Geoquímica de Aguas en Cuencas Cerradas: I, II y III Regiones-Chile*; Ministerio de Obras Públicas, Dirección General de Aguas: Santiago, Chile, 1999; p. 296.
83. Grosjean, M. Paleohydrology of the Laguna Lejía (north Chilean Altiplano) and climatic implications for late-glacial times. *Palaeogeogr. Palaeoclimatol. Palaeoecol.* **1994**, *109*, 89–100. [CrossRef]
84. Anderson, M.; Low, R.; Foot, S. Sustainable groundwater development in arid, high Andean basins. *Geol. Soc. Lond. Spec. Publ.* **2002**, *193*, 133–144. [CrossRef]
85. Montgomery, E.L.; Rosko, M.J.; Castro, S.O.; Keller, B.R.; Bevacqua, P.S. Interbasin underflow between closed Altiplano basins in Chile. *Ground Water* **2003**, *41*, 523–531. [CrossRef]
86. Herrera, C.; Urrutia, J.; Jódar, J.; Lambán, L.J.; Gamboa, C. Investigaciones hidrogeológicas en la laguna Tuyajto perteneciente a la Reserva Nacional de los Flamencos (Atacama, Chile). *Boletín Geológico y Minero.* **2019**, *130*, 789–806. [CrossRef]
87. Urrutia, J.; Herrera, C.; Custodio, E.; Jódar, J.; Medina, A. Groundwater recharge and hydrodynamics of complex volcanic aquifers with a shallow saline lake: Laguna Tuyajto, Andean Cordillera of northern Chile. *Sci. Total Environ.* **2019**, *697*, 134116. [CrossRef]
88. Herrera, C.; Custodio, E.; Chong, G.; Lambán, L.J.; Riquelme, R.; Wilke, H.; Jódar, J.; Urrutia, J.; Urqueta, H.; Sarmiento, A.; et al. Groundwater flow in a closed basin with a saline shallow lake in a volcanic area: Laguna Tuyajto, northern Chilean Altiplano of the Andes. *Sci. Total Environ.* **2016**, *541*, 303–318. [CrossRef]
89. Burri, E.; Petitta, M. Runoff drainage, groundwater exploitation and irrigation with underground channels in Cappadocia: Meskendir Valley case-study. *J. Cult. Herit.* **2005**, *6*, 191–197. [CrossRef]
90. Viaroli, S.; Mastrorillo, L.; Mazza, R. Contribution of the Roccamonfina caldera to the basal volcanic aquifer recharge: First considerations. *Rend. Online Soc. Geol. Ital.* **2016**, *41*, 95–98. [CrossRef]
91. Corriols, M.; Ryom Nielsen, M.; Dahlin, T.; Christensen, N.B. Aquifer investigations in the León-Chinandega plains, Nicaragua, using electromagnetic and electrical methods. *Near Surf. Geophys.* **2009**, *7*, 413–426. [CrossRef]

92. Valentine, G.A.; Graettinger, A.H.; Sonder, I. Explosion depths for phreatomagmatic eruptions. *Geophys. Res. Lett.* **2014**, *41*, 3045–3051. [CrossRef]
93. Graettinger, A.H.; Valentine, G.A. Evidence for the relative depths and energies of phreatomagmatic explosions recorded in tephra rings. *Bull. Volcanol.* **2017**, *79*, 88. [CrossRef]
94. Wohletz, K.H.; Sheridan, M.F. Hydrovolcanic explosions; II, Evolution of basaltic tuff rings and tuff cones. *Am. J. Sci.* **1983**, *283*, 385–413. [CrossRef]
95. Sheridan, M.F.; Wohletz, K.H. Hydrovolcanism: Basic considerations and review. *J. Volcanol. Geotherm. Res.* **1983**, *17*, 1–29. [CrossRef]
96. Kurszlaukis, S.; Lorenz, V. Differences and similarities between emplacement models of kimberlite and basaltic maar-diatreme volcanoes. In *Monogenetic Volcanism*; Németh, K., Carrasco-Núñez, G., Aranda-Gómez, J.J., Smith, I.E.M., Eds.; Geological Society: London, UK, 2017; Volume 446, Chapter 101; pp. 101–122.
97. Cashman, K.V.; Scheu, B. Magmatic Fragmentation. In *The Encyclopedia of Volcanoes*, 2nd ed.; Sigurdsson, H., Houghton, B., McNutt, S.R., Rymer, H., Stix, J., Eds.; Academic Press: Cambridge, MA, USA, 2015; pp. 459–471.
98. Cassidy, M.; Manga, M.; Cashman, K.; Bachmann, O. Controls on explosive-effusive volcanic eruption styles. *Nat. Commun.* **2018**, *9*, 2839. [CrossRef]
99. Valentine, G.A.; Gregg, T.K.P. Continental basaltic volcanoes—Processes and problems. *J. Volcanol. Geotherm. Res.* **2008**, *177*, 857–873. [CrossRef]
100. Parfitt, E.A. A discussion of the mechanisms of explosive basaltic eruptions. *J. Volcanol. Geotherm. Res.* **2004**, *134*, 77–107. [CrossRef]
101. Witte, L.C.; Cox, J.E.; Bouvier, J.E. The Vapor Explosion. *JOM* **1970**, *22*, 39–44. [CrossRef]
102. Büttner, R.; Zimanowski, B. Physics of thermohydraulic explosions. *Phys. Rev. E* **1998**, *57*, 5726–5729. [CrossRef]
103. Zimanowski, B. Phreatomagmatic explosions. In *From Magma to Tephra*; Elsevier: Amsterdam, The Netherlands, 1998; Volume 4, pp. 25–53.
104. Wohletz, K.; McQueen, R.; Morrissey, M. Analysis of fuel-coolant interaction experimental analogs of hydrovolcanism. In *Intense Multiphase Interactions*; Proc US (NSF) Japan (JSPS) Joint Sem: Santa Barbara, CA, USA, 1995; pp. 8–13.
105. Brenna, M.; Cronin, S.J.; Smith, I.E.M.; Sohn, Y.K.; Németh, K. Mechanisms driving polymagmatic activity at a monogenetic volcano, Udo, Jeju Island, South Korea. *Contrib. Mineral. Petrol.* **2010**, *160*, 931–950. [CrossRef]
106. McGee, L.E.; Millet, M.-A.; Smith, I.E.M.; Németh, K.; Lindsay, J.M. The inception and progression of melting in a monogenetic eruption: Motukorea Volcano, the Auckland Volcanic Field, New Zealand. *Lithos* **2012**, *155*, 360–374. [CrossRef]
107. Tchamabé, B.C.; Kereszturi, G.; Németh, K.; Carrasco-Núñez, G. How Polygenetic are Monogenetic Volcanoes: Case Studies of Some Complex Maar-Diatreme Volcanoes. In *Updates in Volcanology-From Volcano Modelling to Volcano Geology*; Németh, K., Ed.; InTech Open: London, UK, 2016; Chapter 13; pp. 355–389.
108. González-Maurel, O.; Godoy, B.; le Roux, P.; Rodríguez, I.; Marín, C.; Menzies, A.; Bertin, D.; Morata, D.; Vargas, M. Magmatic differentiation at La Poruña scoria cone, Central Andes, northern Chile: Evidence for assimilation during turbulent ascent processes, and genetic links with mafic eruptions at adjacent San Pedro volcano. *Lithos* **2019**, *338–339*, 128–140. [CrossRef]
109. Maro, G.; Caffe, P.J.; Romer, R.L.; Trumbull, R.B. Neogene Mafic Magmatism in the Northern Puna Plateau, Argentina: Generation and Evolution of a Back-arc Volcanic Suite. *J. Petrol.* **2017**, *58*, 1591–1617. [CrossRef]
110. McGee, L.E.; Brahm, R.; Rowe, M.C.; Handley, H.K.; Morgado, E.; Lara, L.E.; Turner, M.B.; Vinet, N.; Parada, M.-Á.; Valdivia, P. A geochemical approach to distinguishing competing tectono-magmatic processes preserved in small eruptive centres. *Contrib. Mineral. Petrol.* **2017**, *172*, 44. [CrossRef]
111. Ross, P.-S.; Delpit, S.; Haller, M.J.; Németh, K.; Corbella, H. Influence of the substrate on maar–diatreme volcanoes—An example of a mixed setting from the Pali Aike volcanic field, Argentina. *J. Volcanol. Geotherm. Res.* **2011**, *201*, 253–271. [CrossRef]
112. Lefebvre, N.S.; White, J.D.L.; Kjarsgaard, B.A. Unbedded diatreme deposits reveal maar-diatreme-forming eruptive processes: Standing Rocks West, Hopi Buttes, Navajo Nation, USA. *Bull. Volcanol.* **2013**, *75*. [CrossRef]
113. Valentine, G.A. Shallow plumbing systems for small-volume basaltic volcanoes, 2: Evidence from crustal xenoliths at scoria cones and maars. *J. Volcanol. Geotherm. Res.* **2012**, *223–224*, 47–63. [CrossRef]
114. Ross, P.-S.; White, J.D.L. Debris jets in continental phreatomagmatic volcanoes: A field study of their subterranean deposits in the Coombs Hills vent complex, Antarctica. *J. Volcanol. Geotherm. Res.* **2006**, *149*, 62–84. [CrossRef]

115. Auer, A.; Martin, U.; Németh, K. The Fekete-hegy (Balaton Highland Hungary) "soft-substrate" and "hard-substrate" maar volcanoes in an aligned volcanic complex–Implications for vent geometry, subsurface stratigraphy and the palaeoenvironmental setting. *J. Volcanol. Geotherm. Res.* **2007**, *159*, 225–245. [CrossRef]
116. Rutherford, M.J. Magma Ascent Rates. *Rev. Mineral. Geochem.* **2008**, *69*, 241–271. [CrossRef]
117. Sosa-Ceballos, G.; Macías, J.L.; García-Tenorio, F.; Layer, P.; Schaaf, P.; Solís-Pichardo, G.; Arce, J.L. El Ventorrillo, a paleostructure of Popocatépetl volcano: Insights from geochronology and geochemistry. *Bull. Volcanol.* **2015**, *77*, 91. [CrossRef]
118. Jankovics, M.É.; Sági, T.; Astbury, R.L.; Petrelli, M.; Kiss, B.; Ubide, T.; Németh, K.; Ntaflos, T.; Harangi, S. Olivine major and trace element compositions coupled with spinel chemistry to unravel the magmatic systems feeding monogenetic basaltic volcanoes. *J. Volcanol. Geotherm. Res.* **2019**, *369*, 203–223. [CrossRef]
119. Mattioli, M.; Renzulli, A.; Menna, M.; Holm, P.M. Rapid ascent and contamination of magmas through the thick crust of the CVZ (Andes, Ollagüe region): Evidence from a nearly aphyric high-K andesite with skeletal olivines. *J. Volcanol. Geotherm. Res.* **2006**, *158*, 87–105. [CrossRef]
120. Rutherford, M.J.; Hill, P.M. Magma ascent rates from amphibole breakdown: An experimental study applied to the 1980-1986 Mount St. Helens eruptions. *J. Geophys. Res. Solid Earth* **1993**, *98*, 19667–19685. [CrossRef]
121. Browne, B.; Gardner, J. The influence of magma ascent path on the texture, mineralogy, and formation of hornblende reaction rims. *Earth Planet. Sci. Lett.* **2006**, *246*, 161–176. [CrossRef]
122. De Angelis, S.H.; Larsen, J.; Coombs, M.; Dunn, A.; Hayden, L. Amphibole reaction rims as a record of pre-eruptive magmatic heating: An experimental approach. *Earth Planet. Sci. Lett.* **2015**, *426*, 235–245. [CrossRef]
123. de Silva, S.L.; Riggs, N.R.; Barth, A.P. Quickening the Pulse: Fractal Tempos in Continental Arc Magmatism. *Elements* **2015**, *11*, 113–118. [CrossRef]
124. Godoy, B.; McGee, L.; González-Maurel, O.; Rodríguez, I.; le Roux, P.; Morata, D.; Menzies, A. Upper crustal differentiation processes and their role in 238U-230Th disequilibria at the San Pedro-Linzor volcanic chain (Central Andes). *J. S. Am. Earth Sci.* **2020**, *102*, 102672. [CrossRef]
125. Araya Vargas, J.; Meqbel, N.M.; Ritter, O.; Brasse, H.; Weckmann, U.; Yáñez, G.; Godoy, B. Fluid Distribution in the Central Andes Subduction Zone Imaged With Magnetotellurics. *J. Geophys. Res. Solid Earth* **2019**, *124*, 4017–4034. [CrossRef]
126. Le Maitre, R.W.; Bateman, P.; Dudek, A.; Keller, J.; Lameyre, J.; Le Bas, M.J.; Sabine, P.A.; Schmid, R.; Sorensen, H.; Strekeisen, A.; et al. *A Classification of Igneous Rocks and Glossary of Terms: Recommendations of the International Union of Geological Sciences, Subcommission on the Systematics of Igneous Rocks*; International Union of Geological Sciences: Oxford, UK, 1989; p. 193.
127. Peccerillo, A.; Taylor, S.R. Geochemistry of eocene calc-alkaline volcanic rocks from the Kastamonu area, Northern Turkey. *Contrib. Mineral. Petrol.* **1976**, *58*, 63–81. [CrossRef]
128. Sun, S.-S.; McDonough, W.F. Chemical and isotopic systematics of oceanic basalts: Implications for mantle composition and processes. *Geol. Soc. Lond. Spec. Publ.* **1989**, *42*, 313–345. [CrossRef]
129. Wörner, G.; Hammerschmidt, K.; Henjes-Kunst, F.; Lezaun, J.; Wilke, H. Geochronology (40Ar/39Ar, K-Ar and He-exposure ages) of Cenozoic magmatic rocks from Northern Chile (18–22° S): Implications for magmatism and tectonic evolution of the central Andes. *Rev. Geológica De Chile* **2000**, *27*, 205–240.
130. Wörner, G.; Moorbath, S.; Horn, S.; Entenmann, J.; Harmon, R.S.; Davidson, J.P.; Lopez-Escobar, L. Large- and Fine-Scale Geochemical Variations Along the Andean Arc of Northern Chile (17.5°–22° S). In *Tectonics of the Southern Central Andes: Structure and Evolution of an Active Continental Margin*; Reutter, K.-J., Scheuber, E., Wigger, P.J., Eds.; Springer: Berlin/Heidelberg, Germany, 1994; pp. 77–92.
131. Davidson, J.P.; Harmon, R.S.; Wörner, G. The source of central Andean magmas; Some considerations. In *Andean Magmatism and Its Tectonic Setting*; Geological Society of America: Boulder, CO, USA, 1991; Volume 265, p. 233.
132. Kerr, A.C.; Kempton, P.D.; Thompson, R.N. Crustal assimilation during turbulent magma ascent (ATA); new isotopic evidence from the Mull Tertiary lava succession, N.W. Scotland. *Contrib. Mineral. Petrol.* **1995**, *119*, 142–154. [CrossRef]
133. Huppert, H.E.; Stephen, R.; Sparks, J. Cooling and contamination of mafic and ultramafic magmas during ascent through continental crust. *Earth Planet. Sci. Lett.* **1985**, *74*, 371–386. [CrossRef]

134. Moorbath, S.; Thompson, R.N. Strontium Isotope Geochemistry and Petrogenesis of the Early Tertiary Lava Pile of the Isle of Skye, Scotland, and other Basic Rocks of the British Tertiary Province: An Example of Magma—Crust Interaction. *J. Petrol.* **1980**, *21*, 295–321. [CrossRef]
135. Davidson, J.P.; de Silva, S.L. Late Cenozoic magmatism of the Bolivian Altiplano. *Contrib. Mineral. Petrol.* **1995**, *119*, 387–408. [CrossRef]
136. Risse, A.; Trumbull, R.B.; Kay, S.M.; Coira, B.; Romer, R.L. Multi-stage Evolution of Late Neogene Mantle-derived Magmas from the Central Andes Back-arc in the Southern Puna Plateau of Argentina. *J. Petrol.* **2013**, *54*, 1963–1995. [CrossRef]
137. Maro, G.; Caffe, P.J. The Cerro Bitiche Andesitic Field: Petrological diversity and implications for magmatic evolution of mafic volcanic centers from the northern Puna. *Bull. Volcanol.* **2016**, *78*, 51. [CrossRef]
138. Taussi, M.; Godoy, B.; Piscaglia, F.; Morata, D.; Agostini, S.; Le Roux, P.; Gonzalez-Maurel, O.; Gallmeyer, G.; Menzies, A.; Renzulli, A. The upper crustal magma plumbing system of the Pleistocene Apacheta-Aguilucho Volcanic Complex area (Altiplano-Puna, northern Chile) as inferred from the erupted lavas and their enclaves. *J. Volcanol. Geotherm. Res.* **2019**, *373*, 179–198. [CrossRef]
139. Michelfelder, G.S.; Feeley, T.C.; Wilder, A.D. The Volcanic Evolution of Cerro Uturuncu: A High-K, Composite Volcano in the Back-Arc of the Central Andes of SW Bolivia. *Int. J. Geosci.* **2014**, *5*, 1263. [CrossRef]
140. Tibaldi, A.; Corazzato, C.; Rovida, A. Miocene–Quaternary structural evolution of the Uyuni–Atacama region, Andes of Chile and Bolivia. *Tectonophysics* **2009**, *471*, 114–135. [CrossRef]
141. Filipovich, R.; Báez, W.; Bustos, E.; Villagrán, A.; Chiodi, A.; Viramonte, J. Eruptive styles related to the monogenetic mafic volcanism of Pasto Ventura region, Southern Puna, Argentina. *Andean Geol.* **2019**, *46*, 300–335. [CrossRef]
142. Wohletz, K.; Zimanowski, B.; Büttner, R. Magma-water interactions. In *Modeling Volcanic Processes: The Physics and Mathematics of Volcanism*; Cambridge University Press: Cambridge, UK, 2013; pp. 230–257.